September 2020
Volume 18 Issue 22

Journal of nde
Non Destructive Testing and Evaluation

An Official Journal of the Indian Society for Non Destructive Testing

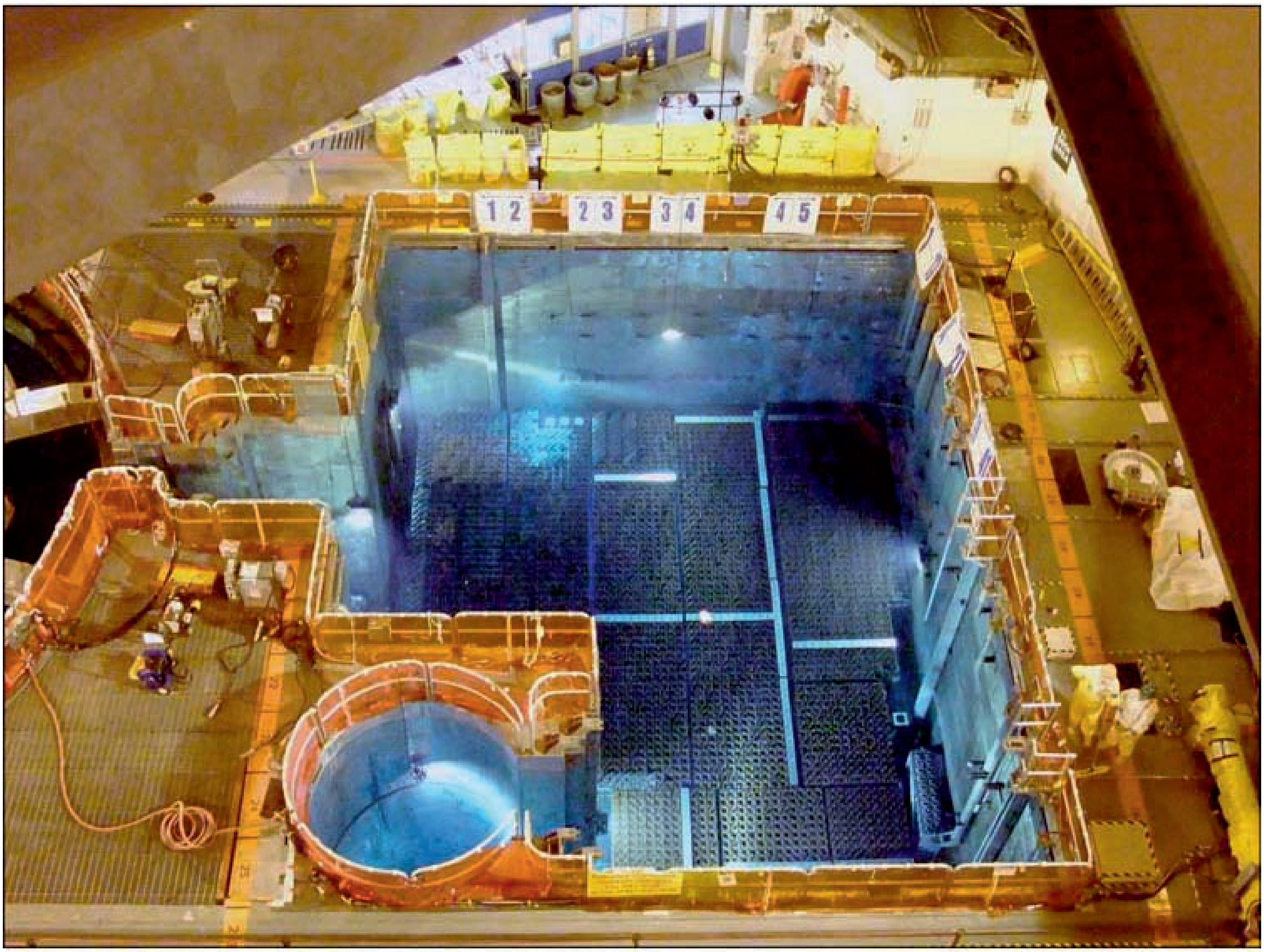

If Undelivered Return To :

Indian Society For Non-Destructive Testing
Module Nos.60 & 61,
Readymade Garment Complex,
Sidco Industrial Estate,
Guindy, Chennai-600032.
Tel: 044-22500412

An ISNT Publication

www.isnt.in

Indian Society for
ISNT
Non Destructive Testing

Contents

Journal of Non Destructive Testing and Evaluation
"Connecting NDT Professionals"
AN ISNT PUBLICATION

SEPTEMBER 2020
Volume 18 - Issue 22

ON THE **COVER** Page

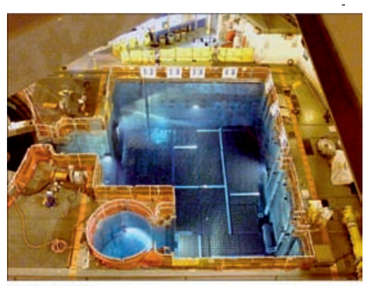

See article (page 11)
Eddy current array for fuel rod inspections and Beyond

OBJECTIVE – This Journal of Non Destructive Testing & Evaluation (JNDE) is published quarterly by the Indian Society for Non Destructive Testing (ISNT) for promoting NDT Science & Technology. The objective of this journal is to provide a forum for dissemination of knowledge in NDE & related fields. Papers will be accepted on the basis of their contribution to the growth of NDE Science & Technology.

PUBLISHED BY:- Mr. Rajul R. Parikh - Managing Editor, JNDE

For JNDE SUBSCRIPTION, NEW / RENEWAL OF ISNT MEMBERSHIP INQUIRIES CONTACT:-
Indian Society for Non-Destructive Testing (ISNT)
Modules 60 & 61, 3rd Floor, Readymade Garment Complex, SIDCO Industrial Estate,
Guindy, Chennai – 600 032. India
Tel: 044-2250 0412 / 4203 8175 ***Email: isntheadoffice@gmail.com, info@isnt.in***

For ADVERTISEMENT INQUIRIES CONTACT:-
Rachna Jhaveri - JNDE Executive
8, Jyoti Wire House, 2nd Floor, Off Veera Desai Road, Near Kolsite,
Andheri (W), Mumbai – 400 053. India
Tel : 022 6150 3839 ***Email : isnt.jnde@gmail.com***

LETTERS

PRESIDENT Talk

Dr. B. Venkatraman
President - ISNT
president@isnt.in

Hope you, your family members and colleagues are keeping safe. With the Covid-19 pandemic showing signs of decline, we hope that things would start tending towards normalization. However, one should not slacken w.r.t precautions.

Though initially the activities at various Chapters and HO were affected during the peak periods from April – August, we could restart connecting with the members through the webinars. I thank members present for sparing their valuable time to join the virtual meetings of NGC, Past Presidents' Meet, 8th Chapter Chairman Meet, and the Webinars organised by ISNT Chapters and also HO.

Both in the past presidents meet and also NGC it has been reiterated that ISNT should hold its flagship event "Conference & Exhibition on Non-Destructive Evaluation (NDE 2020)" as a virtual one during Dec. 10-12, 2020. Accordingly the Central Conference Committee has been vested with the responsibility of organizing this event. Keeping the world wide trends in view, the theme of NDE 2020 has been aptly chosen as "Redefining Industry Parlance with NDE 4.0". The conference focuses on a range of scientific, technological and engineering aspects related to materials evaluation, Condition Monitoring, Codes, Standards, Training, Certification and thematic sessions on advanced topics such as Digital imaging, signal analysis, AI and deep learning. A virtual exhibition has also been planned and as in the past, we would be having a blend of international and national invited speakers. I request all Chapters to disseminate this information to all members so that we can have a large participation.

I thank all of you for your support and look forward to seeing you in NDE 2020 online.

Dr. B. Venkatraman
President

ABOUT ISNT

Indian Society For Non Destructive Testing (ISNT) was formed on 21st April 1989 by merger of two societies namely Non Destructive Testing Society of India registered in Calcutta in July 1972 and Non Destructive Inspection Engineering registered at Madras in March 1981. It is a non-profit organization and is registered under the Tamil Nadu Societies, Registration Act, 1975 (Tamil Nadu Act 27 of 1975) Regd. No.49 of 1981.

The Indian Society for Non-destructive Testing (ISNT) is the society for NDT professionals and practitioners which offers invaluable resources, information and linkages for industrial quality development and professional development to its members. The objective of the Society is to promote the awareness of NDT Science and Technology through education, research and exchange of technical information within the country and internationally to its members and other professionals using NDT. The family of ISNT has more than 6000 strong members. It is a diverse and dynamic family of professionals representing NDT technicians, scientists, engineers, researchers, manufacturers and academicians – all dedicated to improve product safety and reliability. These specialists represent virtually every industry and discipline that may benefit from NDT technology.

ISNT holds periodic seminars and workshops on topics relating to NDT methods and applications, as well as exhibitions displaying cutting edge NDT products and services.

ISNT has 18 chapters spread all over the country with headquarters at Chennai. In addition to the above, we have two wings.

• **National Certification Board** - The National Certification Board has been formed for the training and certification of NDT professionals in India and has been periodically conducting Level-I and Level-II courses through ISNT chapters. NCB-ISNT has been recognized by ASNT as the NSO in India and has been periodically conducting Level III ASNT exams right from 1986. NCB-ISNT plays key role in international harmonization of training and certification.

• **QUNEST – Quality Through Non-Destructive Evaluation Science and Technology** - The QUNEST trust has been formed to : a) Identify NDE issues and thrust areas;
b) Foster NDE Science and Technology nationally with international inputs;
c) Continuing Education and
d) Enhance international standing and make ISNT a global player.

ISNT keeps the members informed about technological advances, new products, certification and training and international linkages.

PUBLICATIONS FROM ISNT

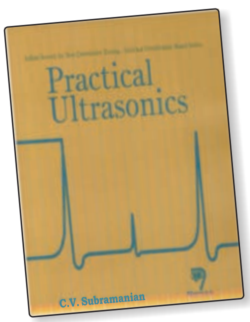

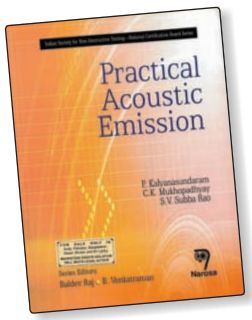

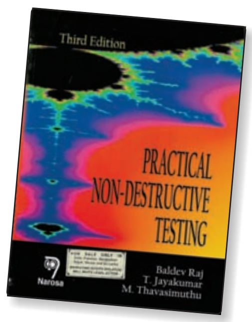

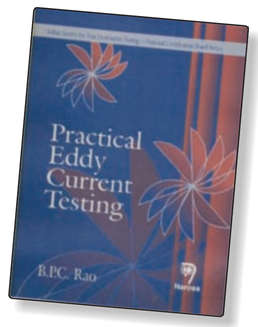

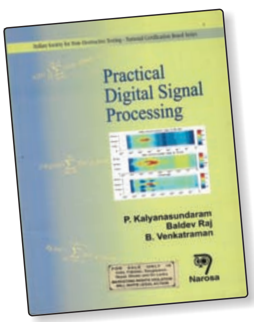

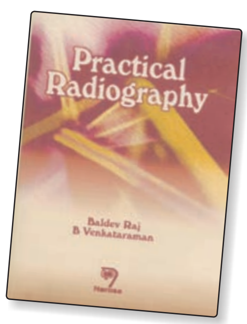

CONTACT:-
MR. VENKAT
Indian Society for Non-Destructive Testing (ISNT)
Modules 60 & 61, 3rd Floor,
Readymade Garment Complex, SIDCO Industrial Estate,
Guindy, Chennai – 600 032. India
Tel: 044 - 2250 0412 / 4203 8175
Email: isntheadoffice@gmail.com

CHAPTER Chairmen & Secretary

AHMEDABAD CHAPTER
Shri. Deepak Parikh **(Chairman)**
Modsonic Instruments Mfg. CO.P. Ltd,
Chairman& Managing Director,Plot no:33, Phase III,
GIDC Industrial Area, Naroda,
Ahmedabad-382330
Ph: 0'98240 27282
deepak@modsonic.com

Shri.Hemant Kumar **(Hon.Secretary)**
Reliance Industries Ltd
VP-CES, Jamnagar-361142
Ph: 0'9998215033
hemantk.kumar@ril.com / hemant.ril2013@gmail.com

BANGALORE CHAPTER
Shri. Sreelal Sridhar **(Chairman)**
Outstanding Scientist & Associate Director.
GTRE,DRDO, Govt. of India, Ministry of Defence,
C.V.Raman Nagar,
Bangalore-560093
Ph :0 9980016442
sreelal@gtre.drdo.in

Shri. Shashidhar P. Pallaki **(Hon. Secretary)**
CEO, Pallakki NDT Excellence Center
No-411, A, 4th Phase, Peenya Industrial Area
Banaglore - 560058
Ph: 0 9448060717
pallakki@pallakkindt.com

CHENNAI CHAPTER
Mr. G. Ramachandran **(Chairman)**
Chairman, ISNT Chennai Chapter
New No.8, Old No: 25, Desi Colony, 3rd Street,
Mangalapuram, Perambur,
Chennai – 600 012.
Phone: 0 9600137919
Email: gr2489@rediffmail.com

Shri R. Vivek (**Hon. Secretary)**
Managing Partner, Electro-Magfield Controls & Services.
"Plot No.165, Women's Industrial Park,
Sidco Industrial Estate," Vellanur,
Kattur Village, Chennai – 600 062
Ph : 0 9840023015
emcs@vsnl.net / r_vivekh@yahoo.com

COIMBATORE CHAPTER
Shri P.Murali (**Chairman)**
Ph: 0 9443491823
muralinaveen@yahoo.co.in

Shri A. Rathinam **(Hon.Secretary)**
Ph: 0'9843011031
everestndt@gmail.com

DELHI CHAPTER
Shri R.K. Singh (**Chairman)**
Ph: 0 9312433853
rajinspection001@gmail.com

Shri F. Siddiqui (**Hon. Secretary)**
541/2, Group-I, Hastal, Uttam Nagar,
New Delhi – 110059
Ph : 0 9811466220
isntdelhi@gmail.com / delhindt@yahoo.com

HYDERABAD CHAPTER
Dr. Jaiteerth R. Joshi **(Chairman)**
Project Director LRSAM-IAC Defence R&D Laboratory,
Kanchanbagh, Hyderabad,
Telangana - 500058
Ph :0 9440049272
joshidrdl@gmail.com

Shri. Surya Prakash Gajjalla **(Hon.Secretary)**
CEO, Associated Engineering Services
Block No. 3-5-944/220-221, 2nd Floor, Panchavati Mall
Narayanaguda, Hyderabad
Telangana - 500029
Ph: 0'09885162668
gajjalla@gmail.com

JAMSHEDPUR CHAPTER
Dr. Sarmishtha P Sagar **(Chairman)**
"Senior Principal Scientist & Group Leader
NDE & MM Group,"Advanced Materials & Processes
Division, CSIR-National Metallurgical Laboratory,
Jamshedpur - 831 007
Ph : (O) 0 657 2345023 / (M) 0 9431521144
sarmishtha.sagar@gmail.com / sarmi@nmlindia.org

Dr. A K Panda **(Hon.Secretary)**
akpanda@nmlindia.org

KALPAKKAM CHAPTER
Dr B.P.C. Rao **(Chairman)**
Associate Director & Chief Project Engineer - QA-FRFCF &
Head - QAD, IGCAR, Kalpakkam-603102
Ph : 0 9498313575
bpcrao@igcar.gov.in

Dr. S. Thirunavukkarasu **(Hon. Secretary)**
Scientific Officer-F Non-Destructive Evaluation Division,
MMG Metallurgy and Materials Group IGCAR,
Kalpakkam - 603 102
Ph: 044-27480500 Extn. : 23630
sta@igcar.gov.in

KOCHI CHAPTER
Shri Sathyan V (**Chairman)**
Ph: 0 9446086245
sathyanv@bharatpetroleum.in

Shri Sibi Ignatius (**Hon. Secretary)**
Ph: 0 9446385611
sibiignatius@bharatpetroleum.in

KOLKATA CHAPTER
Shri Dipankar Gautam (**Chairman)**
AB 121, Salt Lake, Kolkata – 700 064
Ph: 98048 13030 / 98302 03223
dgautam1956@gmail.com

Shri Chandrachudha Bhattacharyya **(Hon Secretary)**
28/2,Satchasi Para Lane,
Kolkata-700036
Ph: 09830251375
chandrachudha@yahoo.co.in

KOTA CHAPTER
Shri Ambresh Bahl (**Chairman)**
CE(QA), RR Site, NPCIL,
PO - Anushakti, Via - Kota, Rajasthan - 323 307
Ph.0 9413351764
abahl@npcil.co.in

Shri A. Varshney (**Hon. Secretary)**
Sr. Engg. (Quality Assurance), RAPS-5&6,NPCIL,
Anu Shakti, Rawatbhata, Distt.Chittorgarh.
Rajasthan - 323303
Ph :0 9413358365
abhishekvarshney@npcil.co.in

MUMBAI CHAPTER
Dr. Paritosh Nanekar **(Chairman)**
Quality Assurance Division, BARC,
Trombay, Mumbai – 400 085.
Ph: 0 9892161750
paritoshn@yahoo.com

Shri Samir K. Choksi (**Hon. Secretary)**
Choksi Imaging Ltd., 4 & 5, Western India House,
Sir P. M. Road, Fort,
Mumbai- 400 001
Ph. 0 9821011113
offc@isnt.org, isntmumbai@gmail.com

NAGPUR CHAPTER
Shri Jeevan Ghime **(Chairman)**
M/s. Becquerel Industries Pvt. Ltd.
33, Rishikesh Modern Co-op. Hsg Society,
Ingole Nagar, Wardha Road, Nagpur - 440 005
jeevan@biplndt.com

Shri Parag W. Pathak (**Hon. Secretary)**
M/s. NDT Solutions Saket - Pruthvi Appt, Plot No. A+B,
Second Floor, Surendra Nagar, Nagpur - 440015
Ph : 0 7709047371
paragwpathak@yahoo.com

PUNE CHAPTER
Shri Sunil V Gophan **(Chairman)**
M/s Radiant Quality Services
91/2, Dwarka Kunj, Shop No. 4, Krishna Colony,
Lane No. 10, Paramhans Nagar, Kothrud, Pune - 411 038
Ph: 0 9766642821
chairman@isntpune.org.in

Shri Chintamani Khade **(Hon. Secretary)**
Building No B/11, Flat No 5 & 6,
Popularnagar Warje Malwadi,
Pune - 411 058
Ph: 0 9822752428
secretary@isntpune.org.in

SRIHARIKOTA CHAPTER
Shri V. Kumbakarnan **(Chairman)**
Project Director, SVAB SDSC – SHAR,
Sriharikota – 524124
Ph: 0'9440391963
vkarnan@shar.gov.in

Shri V. Rajasekhar **(Hon. Secretary)**
Sci/Eng.-SD,NDT,SPP, SDSC – SHAR,
Sriharikota – 524124 Ph: 0'9989898932
rajasekhar.v@shar.gov.in

TARAPUR CHAPTER
Shri. N.S. Gulavani **(Chairman)**
Ph :0'9422066789 / 0'9545436000
nsgulavani@npcil.co.in

Shri Chetan Mali **(Hon. Secretary)**
Scientific Assistant 'F' Quality Assurance Section,
Tarapur Atomic Power Station 1&2,
NPCIL.
Ph :9420304188 / 8806515204
mali.chetan@rediffmail.com

TRICHY CHAPTER
Shri. Revisankaran. U (**Chairman)**
General Manager / Quality /BHEL TRICHY -14
ISNT Building, BHEL Main office Road,
Adjacent to Institute of Engineers Building,
Opp. to 79 Building of BHEL, Trichy – 620 014.
Ph: 9489202949
revi@bhel.in

Shri. Dilip Kumar Singh **(Hon.Secretary)**
Ph: 07845462025
dksingh@bhel.in

TRIVANDRUM CHAPTER
Shri. Arumugam M (Chairman)
Group Director, QCNG/SR -LPSC
Valiamala P.O, Thiruvananthapuram-695547
Ph: 09496020097
m_arumugam@lpsc.gov.in / arumugamm@rocketmail.com

Shri Shunmugavel A (Hon. Secretary)
SCI/ENGR SF, QCM/QCG/MME, RFF AREA
VSSC, ISRO P.O.
Thiruvananthapuram - 695022
Ph: 9249562486
isnttvm@gmail.com

VADODARA CHAPTER
Shri. R. Venkatasubramanian **(Chairman)**
"C/o Industrial X-Ray and Allied Radiographers (I) P. Ltd."
C-17 / 78, Krishana Industrial Estate,
Opposite to BIDC, Gorwa,
Vadodara-390 016
Ph : 0 9825244941
chairmanisntvc@gmail.com

Shri. Kashyap Niranjan Bhatt **(Hon.Secretary)**
Rushikesh Engineering Resources.
306, Vrajsiddhi Tower, Market Char Rasta,
Rajmahel Road,
Vadodara-390010,
Ph : 0 9825245886
secretaryisntvc@gmail.com

All Products Designed & MADE IN INDIA

MODSONIC®
(SINCE 1987)

Simplifying **NDT**

30 Years 1987 - 2017

30 Years' of Focused Leadership in Portable ULTRASONIC TESTING EQUIPMENT

NEW! Arjun Series

Ultrasonic Flaw Detector
- Palmtop ● One Hand Operation
- Ultra-light (Weighs 800 grams with the battery)
- High Resolution Display (800 × 480 Pixels)
- USB Disk and Micro SD card slot
- Dynamic DAC, TCG, DGS, AWS ● Square wave pulser
- Measurement Resolution: 0.01MM ● Built-In Continuous Data Recording and Colour Flaw Plotting

da Vinci Delta

IMAGING Ultrasonic Flaw Detector
- B-scan and C-scan for corrosion survey
- TOFD for weld inspection
- High performance flaw detection
- Oxide Scale thickness measurement
- Test range: 2.5mm to 10 meters
- Measurement Resolution: 0.01MM

INDIA'S #1 Einstein-II DGS

Ultrasonic Flaw Detector
- Most popular user friendly series
- More than 5000 units sold worldwide
- Exported to thirty plus countries
- Dynamic DAC ● DGS/AVG
- AWS ● TCG

Arya Series

MULTICHANNEL Ultrasonic Flaw Detector
- 8 or 16 channels with different colours of A-Scan traces ● Handy design ● 7" Display
- Weighs only 2Kgs ● Ideal for integrators of Automatic Ultrasonic Testing Systems

Edison Series

Ultrasonic Thickness Gauges and Velocity Meter
- Different variants and special probes to fulfil various applications ● Supplied more than 6000 units ● Precision type ● With memory storage facility ● High temperature application ● Through coating measurement ● EL backlight for indoor use

Products for Railways

Axle Tester and Rail Testers
- RDSO approved Railway Products
- Axle Tester
- Rail Weld Tester
- Rail Testers
- Sold more than 1000 units to Indian Railways and also exported

Ultrasonic Probes

Standard and Custom Probes
- Wide range of high quality standard and custom probes with Test Certificates
- Customized probes for various applications.

Allied Accessories

Blocks, Cables and Attachments
- Various probe cables ● Standard Reference and Calibration Blocks ● Special Probe wedges and other attachments
- Various types of UT couplants

Scanners and Encoders

EzeeScan-1 and MagMan
- Single and Dual axis scanners
- TOFD and Phased Array Scanners
- String Encoder for B-Scan
- TOFD Scanners upto 8 nos. probes.

MUX-8

8 Channel Multiplexer
- 8 separate channels with individual adjustments
- 16×2 alphanumeric display
- Rechargeable Li-Ion battery
- Weighs 1.8Kgs with battery

Support Services

Repairs, Calibration and AMC Services
- Quick turnaround service
- Component level repairs for cost effectiveness
- Calibration of flaw detectors as per ASTM E317-11, and EN 12668-1
- AMC for all products

Application Lab

- Full-fledged application lab
- Against your sample we provide free "Evaluation Report" for best solution by Ultrasonic NDT.

All Products Conceived, Designed, Developed and Manufactured in India by:

MODSONIC INSTRUMENTS MFG. CO. (P) LTD

Plot No.33,Phase III, GIDC Industrial Estate, Naroda, Ahmedabad-382 330, INDIA,

Tele: +91 (079) 2281 1217, 2281 3131 **Fax:** +91 (079) 2282 0012 **E-mail:** modsonic@modsonic.com

www.modsonic.com

CHAPTER SPACE

CHAPTER News

CHENNAI CHAPTER

- Technical talk on "NDT & RURAL ECONOMY - CASE STUDIES" by Dr. Prabhu Rajagopal, Professor, Department of Mechanical Engineering, IITM, Chennai, was held on 31st May 2020 through Video Conferencing – Google meet.
- Technical talk on "Quality management system for NDT laboratories as per ISO IEC 17025" by Shri. S S ANANTHAN, Lead Assessor certification assessing laboratories to meet the requirement of ISO IEC 17025: 2005. Consultant TryCAE Industrial Engg. Pvt. Ltd., Tiruchirappalli was held on 12th July 2020 through Video Conferencing – Google meet.
- Technical talk on "Key Changes in ASME Sec V" by Shri M L Ganapathi Rao, Senior Surveyor, Inspection Service Line, Lloyd's Register Marine and Inspection Services India LLP, Chennai was held on 26th July 2020 through Video Conferencing – MS Teams.
- Technical talk on "Decoding SNT-TC-1A 2020, in comparison with SNT-TC-1A 2016 and International Standard ISO 9712:2012 - Personnel Qualification and Certification in Non-Destructive Testing" by Shri. K. Kumaran, Managing Director, ANSA Training & Quality Assurance Private Ltd., Chennai on 16th August 2020 through Video Conferencing – MS Teams.
- Technical talk on "Frequency and Eddy Current" by Ms. Navita Gupta, Satyakiran School of NDT, Delhi, was held on 30th August 2020 through Video Conferencing – MS Teams.
- Technical Talk on "Terahertz NDE: Emerging applications and challenges" by Dr. Bala Pesala,Ph.D., Senior Principal Scientist (CSIR),
- Professor(AcSIR), Council of Scientific and Industrial Research (CSIR)Central Electronics Engineering Research Institute (CEERI)
- Chennai, India, was held on 13th September 2020 through Video Conferencing – MS Teams.
- EC Meeting was held on 31st May 2020 & 16th August 2020.

KALPAKKAM CHAPTER

- "Visual Inspection – What An Inspector shall look for" was conducted during September 2020.
- Exclusive website for ISNT Kalpakkam Chapter is under progress.

MUMBAI CHAPTER

ECT LEVEL II Course and Examination Conduct at BARC from 24th june to 3rd July 2020 and Examination on 06th July 2020.Course coordinator was Mr. Arbind Kumar , and Examiner was Mr. Niraj Kumar.

1. Webinar 1/2020 : Date: June 21, 2020; Topic: Significance of Flaws in performance of Engineering Components ; Speaker: Shri. BK Shah.
2. Webinar 02/2020 : Date: June 28, 2020; Topic:Quality improvements through effective welding control.; Speaker: Shri Arvind Sharma.
3. Webinar 03/2020 : Date: July 12, 2020; Topic: An insight into innovations changing the future of NDE and Inspection.; Speaker: By Dr. Shyamsunder Mandayam, Principal, Scientist, GE Researc
4. Webinar 04/2020 : Topic: Concepts and Misconceptions in NDE procedures; Speaker: Shri. D Joshi
5. Webinar 05/2020 : Topic: Resolution in Radiography and Beyond Speaker: Dr. Paresh Vaidy
6. Webinar 06/2020 : Topic: Non – Destructive Evaluation for material Characterization; Speaker: By Dr. Anish Kumar , IGCAR, Kalpakkam

EC Meeting was held on 7th June, 2020 at online Google meet, 31 Members were attended the EC Meeting.

KALPAKKAM CHAPTER

Online Webinar was conducted on NDT Awareness for TE Student of Sharad Institute of Technology College of Engineering, Yadrav - Ichalkaranji on 1st June.

Online technical lecture was conducted on 'Electromagnetic Testing' by Mr. Abinash Behera of Hindustan aeronautics Ltd., SED, Koraput.on 18th June

Online technical lecture on Advanced NDE in RLA of Boiler components by Shri G.C.Deore, former Manager Thermax Ltd.on 2nd August.

Online Technical lecture was conducted on Memorial lecture Late Shri L.M.Tolani by Mr. B.K.Shah on Accreditation of NDT organizations.

Technical Lecture was conducted by Mr. Uday Kale on UT of welds as per AWS D1.1.

EC Meeting -7th EC meeting was conducted on 30th July.

EC Meeting -8th EC meeting was conducted on 29th August.

AGM was conducted on 16th Sept.

Advance NDT Services

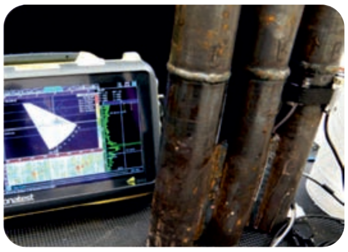

Phased Array Ultrasonic Testing (PAUT)

Thickness Mapping Of
Boiler Tubes With EMAT

High Temperature Thickness Gauging
With EMAT

Remote Visual Inspection/Boroscopy

Tube Testing Solutions
(ECT/RFT/NFT/MFL/ECA)

Corrosion Under Insulation By PECT

NDTS®
NDTS India (P) Limited

NDTS India (P) Limited
619 & 620 The Great Eastern Galleria, Plot No.20, Sector 4, Nerul, Navi Mumbai 400 706
T:+91-22-6138 0600, 2770 3913/23, 2772 9077 | E: info@ndts.co.in | W: www.ndts.co.in

ECT Bobbin Probes & Calibration Tubes

Salient Features

- Coils are potted by a wear resistant material
- Stainless steel wear guides at front & rear ends
- Light weight advance polymer kink-resistant cable
- 4-pin Amphenol connector
- Probes available from 12.6 to 47.6 mm
- Cable length available in 15, 20 & 30 metres

Apart from ECT Bobbin probes we also offer calibration tubes in almost materials as per ASME Sec. V Article 8

ARORA
ISO 9001:2015 Certi?ed Company

Arora Technologies (P) Limited
619 & 620 The Great Eastern Galleria, Plot No.20, Sector 4, Nerul, Navi Mumbai 400 706 India
T: +91 22 6138 0600 | E: info@arorandt.com | W: www.arorandt.com

Eddy Current Array for Fuel Rod Inspections and Beyond: From Manufacturing to End-of-life Management

Anne-Marie Allard[1][0000-0002-8419-9410], Mathieu Bouchard[1], Olivier Rousseau-Cyr[1] and Jitender Yadav[1]
[1]Eddyfi Technologies, 3425, Pierre-Ardouin St. Quebec, Canada
amallard@eddyfi.com

ABSTRACT

The fuel used in Nuclear Power Plants (NPPs) has a long lifecycle, such that it is necessary to establish short- and long-term inspection programs that are essential to ensure workers' and the general population'ssafety as well asoptimal performance of the NPPs during its active life.

Fuel rod integrity assessment – from manufacturing to in-service inspection – is performed to ensure safety and optimal performance of NPPs. Once the rods are removed from the plants and stored, the pools, canisters, and other containment infrastructures are also inspected to ensure proper safety.

Different NDT methods are currently used to inspect fuel rods, canisters, spent fuel pools, and related assets. Each method presents different advantages and limitations, and some are complementary. In terms of surface inspection of rods, canister walls, spent fuel pool welds and other critical parts, conventional eddy current testing (ECT) is often used to detect cracks, pits and corrosion. Unfortunately, ECT is limited in terms of detection, speed, ease of analysis, data recording for future consultation, and ease of deployment.

Advances in electronics has enabled the development of more modern inspection techniques like Eddy Current Array (ECA), increasing reliability, inspection speed through larger coverage, probability of detection, as well as data recording. Being able to tailor coil designs and multiplexing patterns allow users to optimize the acquisition chain to a specific application. Arrays of coils can be packaged in dedicated mechanical casings for specific geometries, made robust for radioactive environments, underwater inspections and more. In addition, by multiplexing and leveraging advanced data processing capabilities, ECA solutions allow inspections to be carried out quickly, often with less surface preparation. Systems available on the market provide additional benefits such as state-of-the-art imaging (e.g. 2D and 3D C-Scan displays), improved surface coverage, ease of deployment anddata archiving. Finally, on top of the increased probability of defect detection, ECA technology can now provide sizing capabilities in some applications.

This paper describes the eddy current array method along with variations on the theme, inclusive of their benefits and limitations. The deployment of actual custom ECA solutions for inspection of fuel rods and containers is also discussed.

Keywords: Non-Destructive Testing, Fuel Rods, Spent Fuel Pools, Eddy Current Array, Dry Canisters

1 Introduction

There are about 450 nuclear power reactors currently in service worldwide, producing approximately 10% of the electricity used. The main contributors are the United States of America, France and China, with a combined production of approximately 1400 TWh [1]. The most common reactor types are the Pressurized Water Reactors (PWR), followed by Boiling Water Reactors (BWR) and Pressurized Heavy Water Reactors (PHWR), also often referred to as CANDU reactors. Each of these reactor types are fueled using rods filled with uranium (mainly) pellets. The fuel rods represent most of a reactor core structure and are a critical component when it comes to the nuclear power plant performance and safety. Their integrity during their entire service life is important to avoid negative impact on reactor operation and plant economics. As the energy produced by the fuel pellets is not infinite, fuel rods need to be removed from the reactor and replaced by new ones. Replacement cycles will vary depending on the plant type, with the most common ones, PWR, having a cycle of about 12 to 18 months [2]. Once the rod's service life is over, the fuel inside is still active and considered as hazardous waste. The level of activity is too low to effectively generate electricity but can still represent a safety and environmental hazard [3]. Consequently, not only is it necessary to ensure rod integrity at the manufacturing and in-service stages, but also prior to its final storage.Care should be taken toward the containers and structures used to store thewaste (e.g.spent fuel pools, canisters, etc.).

The focus of this paper is to introduce eddy current array (ECA) as a new alternative to inspect rods, pools, canisters and other related components to ensure their integrity. Various non-destructive testing techniques are currently used to inspect these parts. Multiple inspection techniques could be replaced efficientlybyECAin order to increase reliability, speed, ease of analysis and ease of deployment. Examples of successful deployment of an ECA system are also discussed to introduce how eddy current array probes can be mechanically tailored to support hightemperature, high radiation and immersion. The capability to design in respect to fluoride, halogen and other specific nuclear limitations as well as the integration with robotic systems is also discussed.

2 Eddy Current Principles

2.1 Conventional Eddy Currents

Eddy current testing (ECT) is part of the inspection methods called non-destructive testing, meaning that the integrity of the component inspected is not altered during the inspection. ECT requires that the probe be in contact (or very close) with the surface inspected, but no couplant is required, gaining some advantage over other techniques, such as ultrasonic testing (UT) for some critical applications and components.

ECT is also what is commonly called a surface inspection technique, meaning that the depth of penetration into the material thickness is limited. Various parameters (frequency, coil diameter, topology, material to be inspected, etc.) can affect the eddy current depth of penetration, but it will often remain limited to the first few millimeters.

Eddy currents are the currents created in a conductive material when an alternating magnetic field induced by a coil close to the surface is created. The technique implies that a copper wire is shaped into a coil and that this coil is excited by an alternating current, which then generates an oscillating magnetic field around the coil. When the coil is brought close to a conductive surface, a magnetic field of equivalent amplitude but opposite direction is created in the material, which consequently induces eddy currents in the material to counterbalance the magnetic field variations. The eddy current direction is opposed to the current induced in the coil.

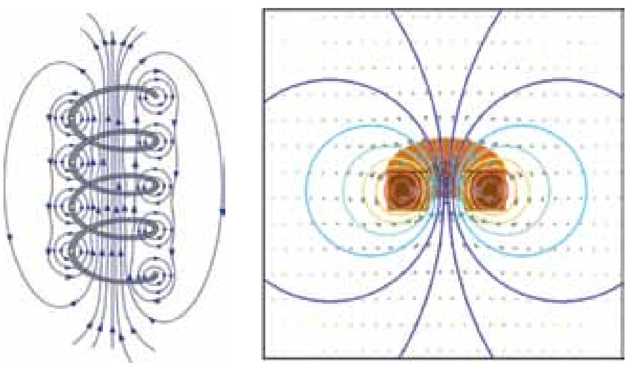

Fig. 1. : Schematization of the magnetic field created in the coil. The magnetic field oscillates at the same frequency as the current injected in the coil

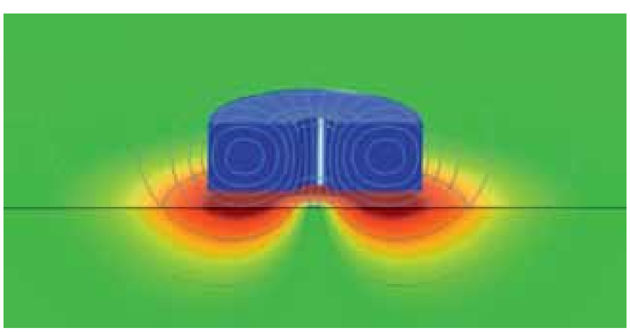

Fig. 2. : Schematization of the induced eddy current in the conductive material

When the coil moves over the inspected surface, the eddy currents will be impacted by the presence of an abnormality in the material. The changes in the eddy current density will then have an impact on the coil impedance. It is the variation of impedance that is measured by the acquisition unit: the amplitude and phase of this variation are displayed in an impedance plan.

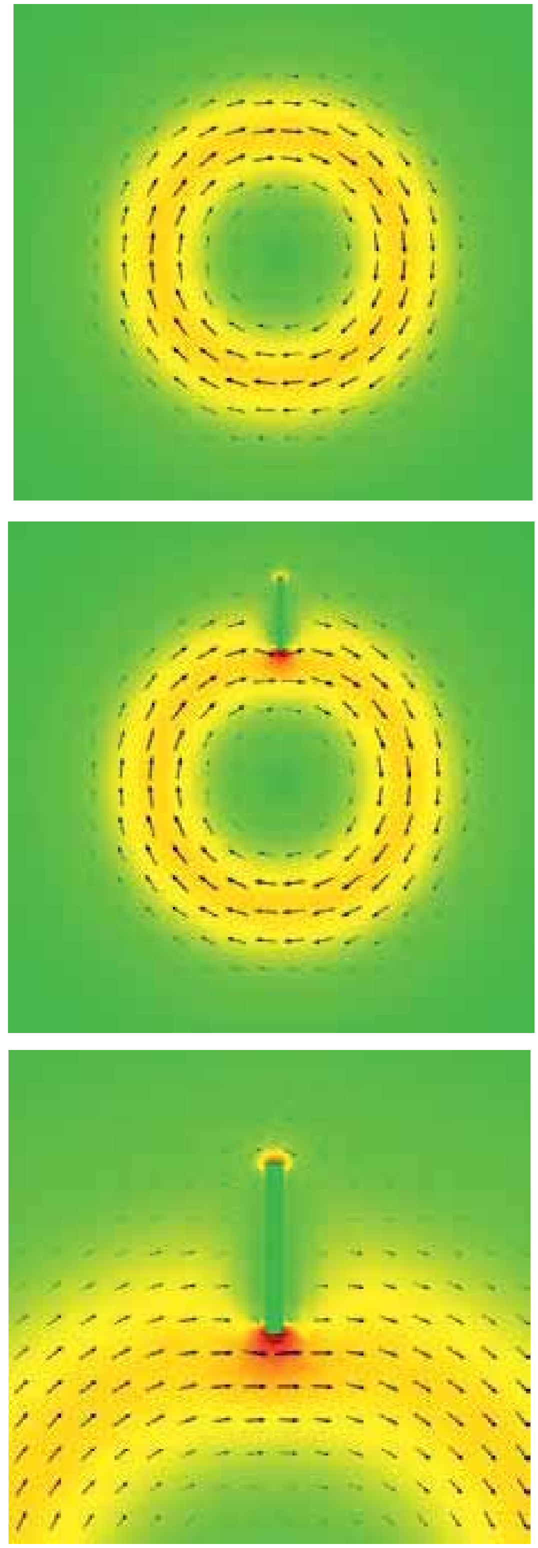

Fig. 3. : Simulation of the impact of a linear indication on the density of eddy current in material

The way the eddy currents are distributed in the conductive material is impacted by various parameters such as: 1) electrical conductivity and permeability of the inspected part; 2) geometry; 3) coil characteristics (wire gage, number of turns, etc.); 4) frequency and drive voltage; 4) lift-off, etc.

ECT is a very sensitive method for surface inspection, and it can be used for various applications such as flaw detection, coating thickness measurement, material sorting, etc. On the other hand, conventional eddy current inspection is highly operator dependent, time consuming on large surfaces, and can be difficult to deploy in remote locations.

2.2 Eddy Current Array

Fundamentals

The fundamentals of ECA are the same as ECT, but with an array of coils packaged in the same assembly. Such an arrangement has numerous benefits including but not limited to:

- Larger coverage, thus increased productivity;
- Capability to inspect hard to reach areas with tailored mechanical packaging allowing for single pass inspection in lieu of complex raster scanning systems;
- Reduced need for complex robotics when automation required;
- Capability to adapt multiplexing patterns and firing sequences to:
  - Improve sensitivity on small indications and/or
  - Reduce sensitivity to lift-off and/or
  - Increase depth of penetration
- Reduced requirements for surface preparation;
- 2D and 3D C-scan imaging;
- Qualitative sizing;

These benefits come from the ability to optimize the firing sequence and multiplexing pattern in order to avoid crosstalk and optimize performance for a given application.

ECA probe optimization

Coils. The coils can be different shapes and sizes. Most commonly in ECA, the shape is similar tothat of a pancake. The copper wire is wound so that the final product looks like a disk. During the design of the coil, different parameters need to be considered:

- Material inspected
- Location of the indication (near side or far side)
- Size of the smallest indication
- Minimum coverage required
- Surface condition such as corrosion
- Lift-off

The above will have an impact on the wire gauge used, number of turns, number of layers, etc. Experts in the fields of ECA are then able to optimize the sensors to offer optimal performance for challenging applications.

Disposition: Thanks to the recent advancements in electronics, it is now possible to optimize the firing sequence of each coil of the array with the possibility of having up to 256 channels in a single probe. The high-channel count of the latest instruments not only allow increases the coverage but can also be used to increase probe sensitivity. For example, for fuel rod inspection, the rod diameter is considered small and the number of coils required to cover the entire circumference is limited. On the other hand, the size of the target indication is also very small, which causes the probability of detection (P.O.D) to fall to low values when using a single row of coils. It was determined, for this development, that the min/max ratio with 2, 4 and 8 (final solution) rows of coils was progressing from 23% to 72% to 92%. Consequently, the firing sequence and number of channels of a probe for fuel rod inspection is optimized to increase the P.O.D. Fig. 4 below illustrates the concept of response curves and the impact of the number of rows.

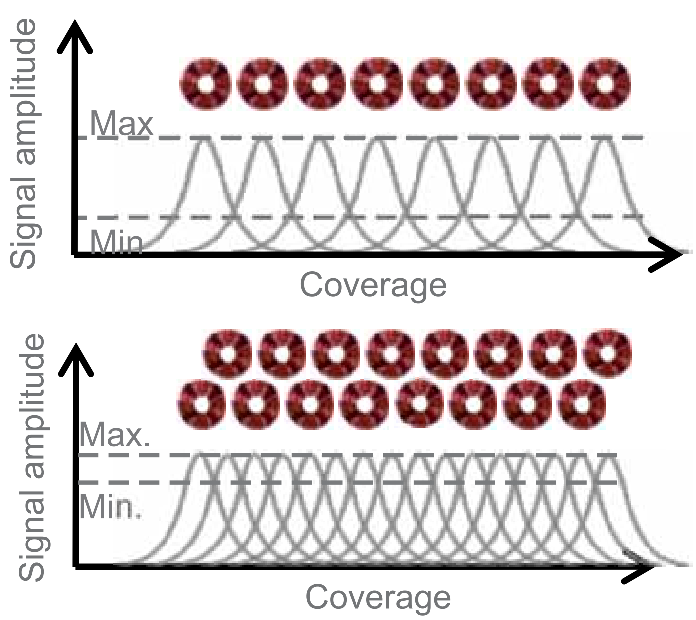

Fig. 4 : Eddy current signal uniformity according to number of rows

Topology: Another advantage of ECA over conventional ECT is the ability to use the coils for different roles at different times in the multiplexing sequence. At some point during the scan, an element can be used as a driver and then later as a receiver. The topologies can be separated in two main groups, the first one being impedance bridge and the latter being Transmit-Receive (T-R).

A channel that is considered absolute will be sensitive to indications in all orientations. A single C-scan image will be displayed, but assessment on the flaw orientation, if linear, is limited if at all possible.

On the opposite, a transmit-receive probe will have two groups of channels, one sensitive to indications parallel to the scan axis (axial indications) and the other being sensitive to indications perpendicular to the scan axis (transverse indications). Both groups are sensitive to oblique and volumetric indications. This type of topology offers more information on the directionality of the indication, as two (2) separate C-scan images are created.

Besides directionality, the main advantages of T-R mode over impedance bridgeis that it is less sensitive to surface finish of the inspected part as well as lift-off. With some T-R topologies, depth of penetration can also be increased if needed.

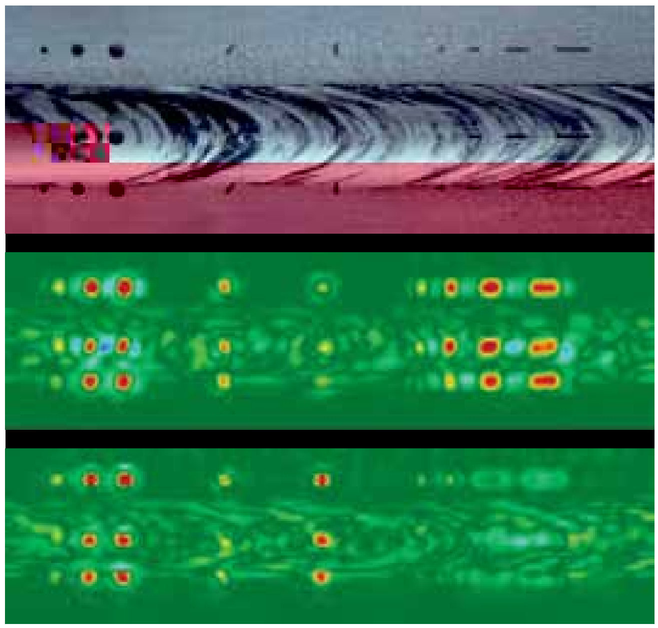

Fig. 5 : Example of ECA C-scan showing directionality of transmit-receive probes

3 Fuel rod inspection

As mentioned in the introduction, fuel rods are a critical component of a nuclear reactor. They are optimized for each type of reactor. For example, PWR requires long rods (total assembly length around 4-5 meters) while PHWR rods are only 50 cm long.The bundling is also different: PWR are arranged in square lattice while PHWR are arranged in circular bundles. Nonetheless, the rods in all type of reactors are of great importance as they hold the fuel, and their integrity has an impact on nuclear power plant (NPP) performance.

Consequently, inspecting rods at the manufacturing stage as well as in service can prove important as it ensures better performance and reduces economic losses.

ECA is renown as a surface inspection, but in the case of fuel claddings, the wall is thin enough that ECA can be used to detect indications on the outside and inside wall of the cladding.

The failure mechanism can be different from one type of reactor to the other, but the most advanced fuel rod probes can detect a wide variety of flaws:

- Axial and circumferential cracking
- Corrosion
- Fretting
- Pitting

The latest high-channel count acquisition units also enable acquisitions with high-resolution probes, allowing for detection of very small indications. The most performant fuel rod probe design can detect the following flaw type and sizes:

- Cracks: 5mm (L) x 0.5mm (W) x 0.11mm (D)
  [0.2 in (L) x 0.02 in (W) x 0.004 in (D)]
- Pitting through wall: ϕ0.25 mm
  [ϕ 0.001 in]
- Sphere (RBH): ϕ 1.5mm x 0.12 mm (D)]
  [ϕ 0.06 in x 0.005 in (D)]

Moreover, the design of this equipment took into consideration the high level of radiation (up to $1X10^6$ RAD/h) present during the inspection and the fact that it was to be deployed underwater. The materials selected to manufacture the probe are radiation and water resistant and their content in fluoride is such that it respects standard regulations.

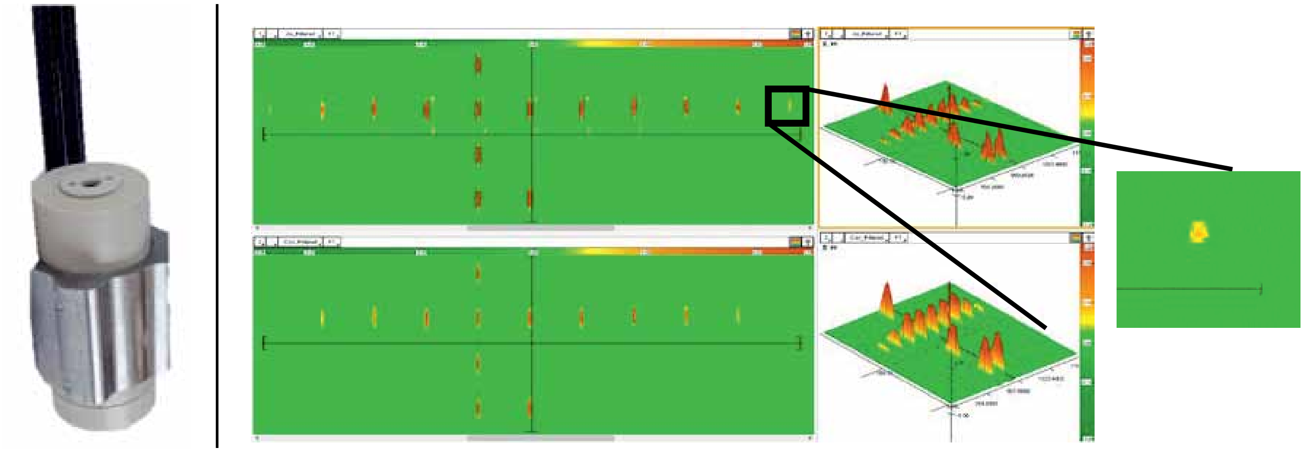

Fig. 6 : Left: Picture of a fuel rod probe assembly for PWR. Right: Typical data display from fuel rod probes – axial and transversal C-scan. 11 indications (cracks and pitting),

4 Spent Fuel Pools

Used fuel from nuclear reactors is considered as Heavy-Level Waste (HLW). Over the years, it has been determined that the best option to dispose of HLW is geological disposal. But prior to burying the used fuel, it is common to store the waste for a period of forty (40) to fifty (50) years above ground so that the level of heat and radioactivity has dropped by 99% of its initial value.

Most of the storage facilities either use storage ponds or dry canisters. Storage ponds are deep pools into which the used fuel is placed and surrounded by water. The water is used as a shield as well as a coolant.

Spent fuel pools are reinforced concrete pools protected by a steel liner. Each piece of liner is welded together. There are also plug welds in the face of the liners. Despite the great care taken in the assembly of these liners, welds remain potential sources of failure and need to be monitored.Upon construction of the spent fuel pool, inspection of the welds is less of a challenge as there are fewer obstacles, but in-service inspection is a different story as the pool is filled with water and used fuel. Consequently, water resistance is required and probe profile must be as low profile as possible in order to fit between the liner and the racks. Also, with the shape of the butt welds between each liner not being constant, flexibility of the reading surface is essential in order to conform to the changing geometry and keep constant contact with the surface (minimize lift-off).

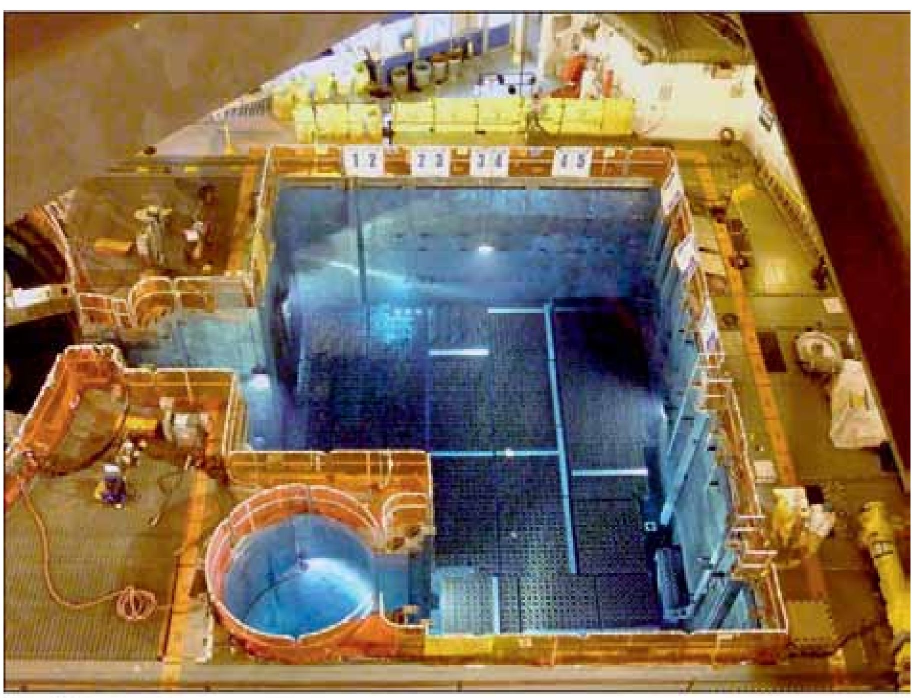

Source: Nuclear Energy Institute.

Fig. 7 : Picture of a filled spent fuel pool. Photo courtesy.

This where a low profile cushioned ECA probe comes in handy to overcome these challenges. The cushioned surface is flexible to ensure an acceptable level of detection in the toe area, but also requires that the coils are protected from water ingress using a flexible but incompressible compound. It is important it resists the pressure variation induced by water without impacting the probe flexibility (up to 51 psi at 25m (82 ft) deep), so that the cushion is not compressed or deformed during immersion.

Fig. 8 : Padded probe design capable of conforming to weld caps up to 5mm high. Provides good detection performance in the toe area.

Another challenge arising for this application is the need for a low-profile probe. As depicted in Fig. 7, the racks of used claddings are stacked close to the wall. Considering the high radiation environment (in the range of 10,000 Rad/h), the deployment is done using a robotized system which must be taken into consideration when designing the eddy current array probe.

Finally, the biggest technical challenge coming from this application is the long cable length required to reach the floor of the pool. When using ECA, a phenomenon called resonance frequency can occur when working with long cable. The relationship between the system impedance (coil, cable and acquisition unit) can be displayed as a curve which varies with the injection frequency. Working at or very close to the resonance frequency shall be avoided as the system is in an unstable state when doing so. Studies and trials were performed in order to optimize detection levels while respecting the physics limits. Fig. 10 below shows how, for the same system, the cable length influences the resonance frequency. Note that the system impedance also varies, as the coil impedance is a function of the injection frequency.

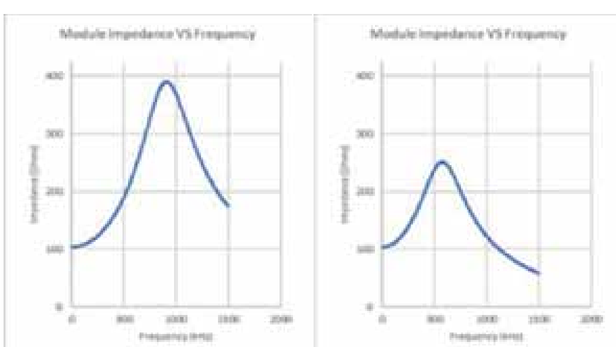

Fig. 9 : Comparison of resonance frequency for 5 m (16.4 ft) and 25 m (6.56 ft) long cables. Same coil inductance and cable capacitance.

5 Dry Canisters

Dry storage of spent fuel is done by placing cooled fuel bundles from a spent fuel pool inside a steel cask. In the case of the project described below, casks were made of stainless steel. The stainless-steel canisters are then enclosed in a ventilated concrete shell, which provides protection against radiation. Usually, the casks are above ground, but some are also partially buried, with only the top showing. The component of interest in this case is once again the conductive material, meaning the stainless-steel cask, and more specifically, the vertical cylinder.

Once again, good contact between the probe and the surface to inspect is essential in this application as well as conformability to compensate for the cylinder manufacturer tolerances and even different diameters of cylinders. In addition to those two requirements, it was necessary to design a probe with the lowest profile possible, as the sole entry into the concrete canister is through a narrow outlet vent. Moreover, profile limitation was important to consider as some rails and other structural features are present between the concrete shell and the steel cask. In some areas, the maximum available space was below 12.7 mm (0.5 in). The probe and the deployment mechanism holding the probe must fit within the outlet vent and below the rails. Such limitation prevents from using a typical rigid casing.

The solution proposed includes a flexible support where the coils are directly connected in order to minimize the space required for cable management over the flexible area. Micro-coaxial connections are deferred further back into a dedicated section that doesn't need to be flexible. The flexible support can adapt to geometry variations and pass over low profile welds. Ground flush welds can be inspected using this solution.

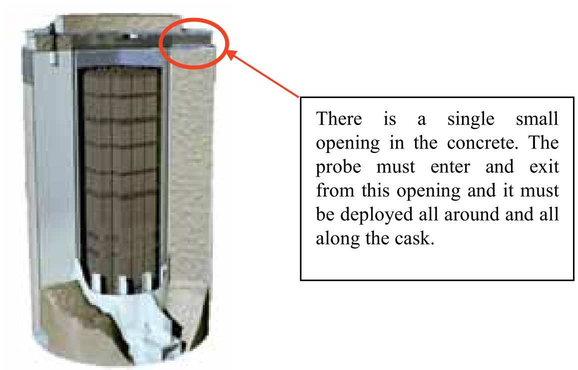

Fig. 10 : Example of a dry canister design. Photo Courtesy.

As for the spent fuel pool application, canister inspections also occur at high temperatures, despite the ventilation system included in the assembly. Radiation level is lower, but still needed to be considered to ensure the probe's longevity.

In terms of detection, the solution offers the benefits of having three embedded topologies, granting capabilities to detect various types of flaws:

- Short and shallow surface-breaking cracks and;
- Long and deep surface-breaking cracks and;
- Subsurface cracks.

6 Conclusion

Nuclear power plants have been in operation for more than 60 years and will remain in the landscape for a while. The quality of cladding used to contain the fuel is important as it can have an impact on safety and performance during the service life of the fuel. Once the fuel pellets are no longer supplying enough energy, they still remain a hazardous waste that needs to be carefully stored. The storage containers used are also critical components that need to be monitored. Eddy current array is a non-destructive testing technique perfectly applicable for such applications, as it can be tailored specifically to optimize detection, coverage, inspection speed and even survive the harsh conditions of inspection (radiation and underwater in some cases). Successful projects to inspect fuel rods, spent fuel pool welds and dry storage canisters have been completed in the past few years, as described above. In addition to these applications, ECA may also be a good inspection technique when it comes to transportation of the fuel, or any other applications where sensitivity to small surface flaws and adaptability to challenging geometry is of essence.

References

1. World Nuclear Association. Nuclear Power in the World Today. *World Nuclear Association.* [Online] September 2019. [Cited: October 10, 2019.] https://www.world-nuclear.org/information-library/current-and-future-generation/nuclear-power-in-the-world-today.aspx.
2. World Nuclear Association. Nuclear Fuel and its Fabrication. *World Nuclear Association.* [Online] June 2019. [Cited: October 10, 2019.] https://www.world-nuclear.org/information-library/nuclear-fuel-cycle/conversion-enrichment-and-fabrication/fuel-fabrication.aspx.
3. —. Radioactive Waste Management. *Worl Nuclear Association.* [Online] April 2018. [Cited: October 10, 2019.] https://www.world-nuclear.org/information-library/nuclear-fuel-cycle/nuclear-wastes/radioactive-waste-management.aspx.

Reliability in Defect Classification and Characterization in Eddy Current Non Destructive Evaluation

Tarun K. Das*, Chandan Dutta, Alok Kumar, S. Palit Sagar
CSIR-National Metallurgical Laboratory, Jamshedpur, India.
*Corresponding Author: Email - tkdas@nmlindia.org

Quantitative assessment of reliability of defect classification and characterization in critical engineering components plays a key role in ensuring the optimal quality control of the finished product. Classification of defect using characteristics functions and extraction of key features using the smart signal analysis tools are indispensable nowadays in order to evaluate the defects alongwith real-time defect detection. This work presents a technical review of Eddy Current (EC) NDE technique in various scope of defect detection. EC testing is widely used for NDE of metallic structures in characterizing numerous types of defects such as sliver, fin, and craw-fit, weld line defect etc occurring in various locations. A framework has been developed for incorporating the Orthogonal Test Method (OTM) in order to increase the sensitivity of the EC sensor for different kind of natural and artificial defects in steel wires. Smart signal analysis and processing toolkit has applied to the EC testing data for characterizing the naturally as well as artificial defects. Furthermore, severities of defects have been identified with this developed framework. The effectiveness of the proposed technique is demonstrated on experimental data from eddy current inspection of defects in high speed drawn steel wires.

Keyword: Orthogonal Test Method (OTM), Eddy Current, Sliver, Fin, Severity of defects, Signal analysis and processing toolkit.

1. Introduction

The eddy current (EC) inspection is extensively used in defect detection and classifications due to its numerous advantages such as rapidity, non-contact mode of operation and it does not require a coupling agent [1–4]. EC testing can find a wide range of defects such as cracks, shells, seams, slivers, pitting, laps, weld-line defect etc. It can assess the criticallity of defects and provides a measure upto what extent it can be acceptable so that optimal quality control is maintained. Hence, quality assurance of engineeting components during their production process itself is a challenging task because tracing of individual defects at a production speed and attempting to find those locations is difficult task as well. In order to address these issues, developments of NDE based protocol along with smart signal analysis tools are indispensable. These issues can be addressed by using eddy current based NDE protocols that can detect, classify and qualify surface defects during production while provide immediate feedback on the product quality - even at production speed. A framework has been developed for incorporating the Orthogonal Test Method (OTM) in order to increase the sensitivity of the EC sensor for different kind of natural and artificial defects in steel wires. Smart signal analysis and processing toolkit has applied to the EC testing data for characterizing the naturally as well as artificial defects. This produces a high demand of non-invasive based defect detection system that can be readily commissioned with the existing machine with small modifications.

Apart from that other main parameter that quantifies the reliability of any NDT inspection techniques is probability of detection (POD) [5]. In general, a good EC testing solution must satisfy the following three requirements: (i) A fast detection of the location of cracks; (ii) Capable of describing the shape of natural cracks and (iii) The algorithm should be robust in the presence of noise in EC signal. For a particular crack reconstruction algorithm the first two aspects many not be clearly related to noise factor but the result of the shape reconstruction can be significantly affects by random noise in the testing signals [6]. Eddy current generated within the metallic parts is the function of alternating magnetic field which couples with it. The frequency of excitation affects the depth of penetration of eddy current. Quantification and classification of surface defects and representing there characteristics is one of the most complex task associated with eddy current inspection. Defects occur in engineering components such as wire/rods are broadly named as sliver, fin, crow feet, longitudinal defects, transverse crack. Exploration of characteristic phenomena observed in coil impedance for other types of defects such as silver, fin craw fit will eventually help to characterize defects in broader scale. The ECT signal characterization can be broadly classified in two ways i. Signal based classification in which Eddy current 1D signal representing sensor resistance and reactance are classified using different regression tools and ii. Shape based classification in which complex sensor coil impedance patterns are classified using neural networks [7].

2. Experimental, Results and Discussions

Defect classification based on signal processing are relatively easier compare to shape based classification as it involves less computation complexity. The characteristic feature that has to be explored for classification and quantification of defects are transient in nature so merely doing Fourier transformation (FT) of the ECT signal will not help to classify and quantify the defects present in wire/rods. Wavelet based transformation techniques are most commonly found in literature as it provides wide range of classifier/wavelet families that helps to extract characteristic feature even from noisy signals. Wavelet based time-frequency transformation requires proper selection of wavelet family to ensure proper extraction of relevant feature without any information loss. Discrete wavelet transform (DWT) with level based thresholding to eliminate noise due to surface irregularity resulting in lift-off variation in boiler vessel pipes [8].The obtained EC signals are decomposed into detail and approximate coefficients through successive high and low pass filtering. The coefficients obtained in each level gives frequency content of the decomposed EC signal at its respective levels which is one of the characteristic feature which are used for signal classification. On the other hand statistical approaches are also practised to eliminate noise from the EC signals. Classifications of noises present in EC signal are of paramount importance for enhancement of detection abilities of anomalies present on sample under test. Noises are modelled using simplistic Gaussian models to design statistical based filtering algorithms to eliminate desired noise from acquired EC signals [9]. Once appropriate filtering of the signal is done variations recorded in signal due to surface abnormalities can be post evaluated for defect characterization using non-linear regression techniques and neural networks [10]. In this work we have tried to extract the relevant features which are obtained both from statistical modelling and wavelet based transformation of raw eddy current signals. Then an appropriate neural network (NN) has been trained with signals obtained for artificially created transverse and longitudinal defects. Selection of appropriate neural network (NN) activation function has been evaluated in this work. The proposed neural network (NN) has been trained over several data sets with different process combinations such as wire/rod drawing speed, lift-off variation, wire/ rod vibration and the type of defects which are developed artificially in pilot scale.

2.1 Sensor/Probe Simulation

A very well practised method for optimizing eddy current sensor probe is orthogonal test method (OTM). The proposed method is purely empirical but at the same time very effective. It reduces the workload of fabrication and increases the efficiency of the sensor probe [11] .

Numerical model are generally developed to optimize coil dimension in several electromagnetic based simulation software. All though the models are extremely closer to actual sensor coils but still certain assumptions has to be made in terms of parasitic, initial and boundary conditions. The models till now developed are static in nature and does not incorporates dynamic evaluation were the sample or sensor coil/coils are in relative motion to each other in simulation. Once the simulation models are evaluated physical sensor has been developed using CNC based micro wire coil winding machine. The use of CNC based winding machine ensures uniform winding maintaining layers. This makes the sensor more identical to its respective simulation design and reduces the deviation in electrical parameters obtain from physical ECT sensor coil and simulation model. The entire probe developed were characterise using 4294A Agilent Impedance analyzer. The dimensional variables taken as factors of OTM are listed in table 1 with its respective values. The dimensional details of the sensor coil designed in ComSol Multi-Physics are listed in table 1 and material parameters used in simulation are listed in table 2.

Table 1 : Details of sensor structure size taken in simulation

Coil Geometry	
Coil Type	Absolute
Wire SWG	28
Wire Diameter	0.376[mm]
Number of Turns	252
Coil ID	5[mm]
Coil OD	11.76[mm]
Coil Length	10[mm]
Wire Material	Copper
wire Electrical Conductivity	6e7[S/m]
Current fed into coil	10[mA]
Frequency of Excitation	50[KHz]

Table 2 : Material parameters used in simulation analysis

Sample Details	
Sample Diameter	2[mm]
Sample Length	20[mm]
Electrical Conductivity	1.12e7[S/m]
Relative Permeability	200
Relative Permittivity	1

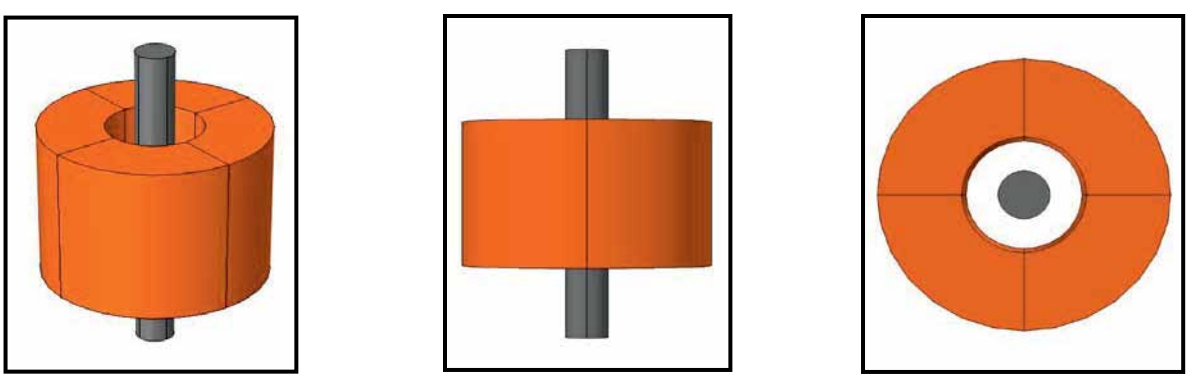

Fig 1a Fig 1b Fig 1c

Fig. 1 : (a) Coil with sample Isometric View; (b) Side View; (c) Top View

2.2 Simulation results

There are two types of defects that have been considered for simulation analysis (longitudinal and transverse defects). Figure 2 shown below shows the CAD representation of the defects considered in simulation model. The defects are varied in size and potential developed accross the terminals of the coils has been evaluated for each case.The results obtained from simulation model with above mentioned sensor and material details are listed in table 3 and 4.

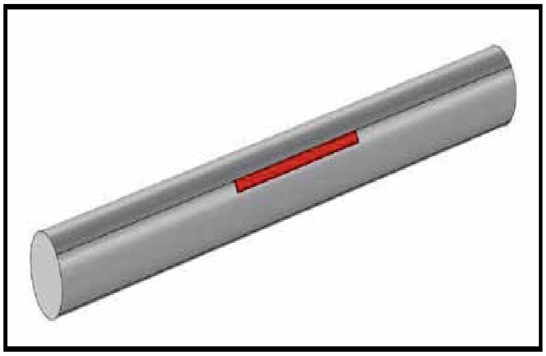

Fig 2a

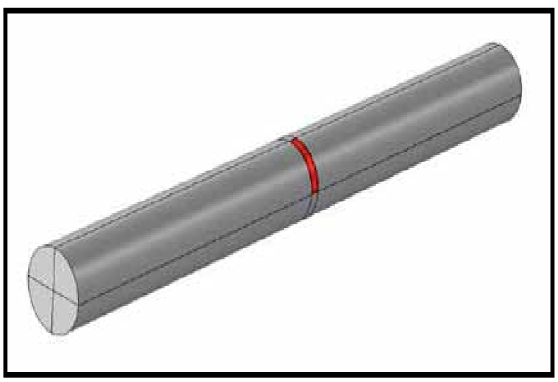

Fig 2b

Fig. 2 : (a) Longitudinal Defect (b) Transverse Defect

Table 3 : Simulation results for longitudinal defects ranging from 100 micron to 500 micron

Sl. No.	Defect Size, micron	Voltage across coil, Volt	Delta mV
1	0	1.0534	
2	100	1.0639	10.50
3	150	1.0665	13.10
4	200	1.068	14.60
5	250	1.0672	13.80
6	300	1.0689	15.50
7	350	1.0733	19.90
8	400	1.0765	23.10
9	450	1.0745	21.10
10	500	1.0808	27.40

Table 4 : Simulation results for transverse defects ranging from 100 micron to 500 micron

Sl. No.	Defect Size, micron	Voltage across coil, Volt	Delta mV
1	0	1.0534	
2	100	1.0669	13.50
3	150	1.0632	9.80
4	200	1.0626	9.20
5	250	1.0643	10.90
6	300	1.0629	9.50
7	350	1.0658	12.40
8	400	1.0648	11.40
9	450	1.0634	10.00
10	500	1.0626	9.20

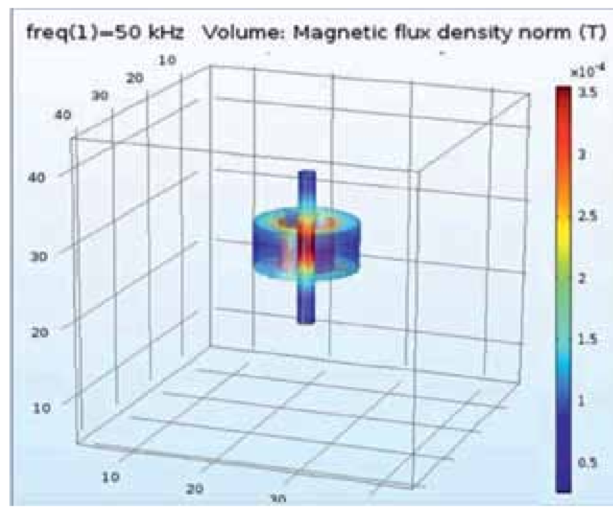

Fig 3 : Simulation result showing normalized magnetic flux density (T) within wire

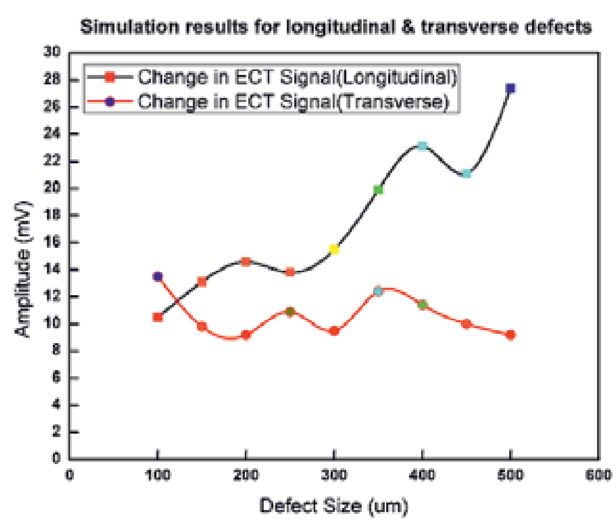

Fig 4 : Plot for change in voltage signal across coil w.r.t to clean sample compare to transverse defects

As one can see that eddy current are more sensitive to longitudinal defect compare to transverse defetc. The coil impedance change shows some trends with the defect size. These observations are purely done on the basis of simulation analysis.

2.3 Experimental result

Physical coil was fabricated with optimized structural parameters obtained from simulation analysis. The sensor is then encapsulated inside a proper housing arrangement fitted with guiding rollers to minimize wire vibration and maintain constant lift-off. The entire inspection system is embedded into a single unit with high speed data acquisition (DAQ) card. The acquired voltage signal across the coils is further amplified to improve its signal to noise ratio (SNR). The amplified ac signal is then converted into its equivalent DC value using modulator/demodulator unit. The final output of the system is scaled in the range of 0 to 10 Volts. The final DC output is ploted in strip mode plotter where straight line signal represent clean defect free wire. The DC signal shows specific peaks with different transient feature when ever a crack of defects passes through the coil. The transient responses are unique for different types of defects. If the speed of wire drawing is known then these transient parameters for defect can be used to evaluate sevearity of different types of surface defects and welds subjected to post signal processing. The below figure 5 shows the mechanical arrangement done at laboratory to simulate the wire drawing process. In the below shown arrangement wire can rotate at varying speed upto few meter per second.

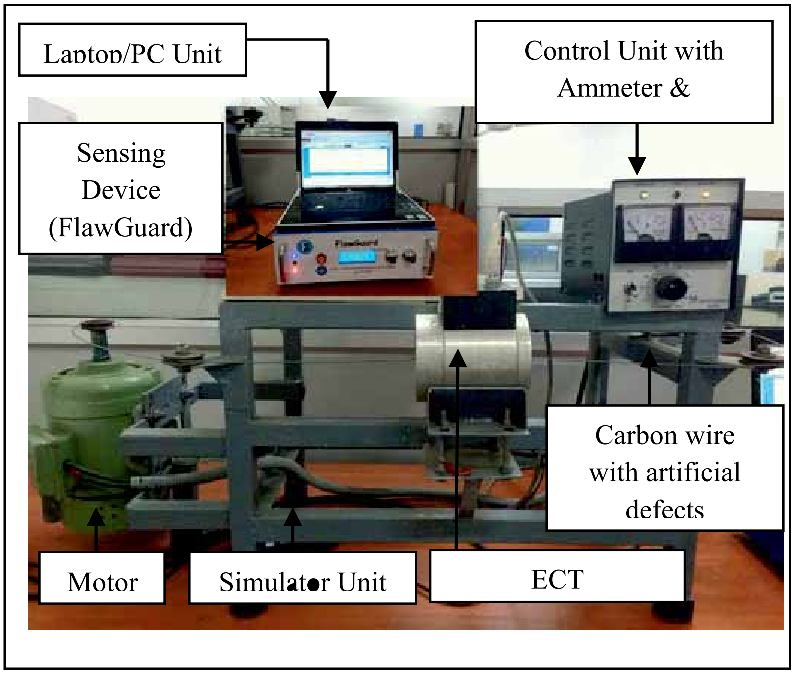

Fig 5 : Experimental setup to detect weld joint using ECT system

The final DC output signal for butt-weld done on 2 mm steel wire has been capture using high speed data acquisition card and recorder over LabView program is shown in figure 6 below.

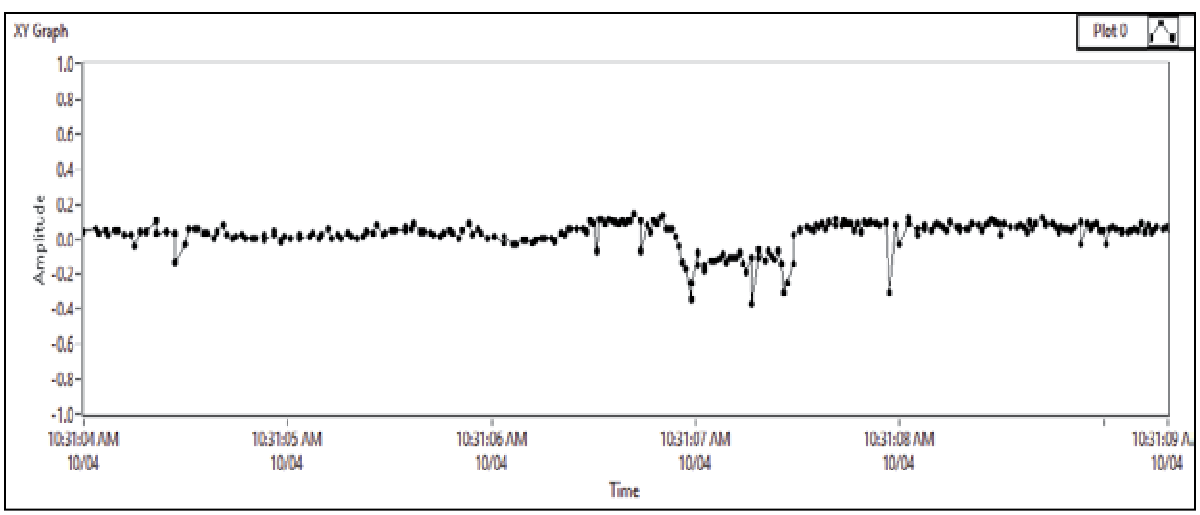

Fig 6 : Weld Signal capture using ECT system

3. Conclusion

A technical review of Eddy Current (EC) NDE technique in various scope of defect detection in high end drawn wires has been demonstrated. A framework using eddy current based NDE protocols was developed that can detect, classify and qualify surface defects during production while provide immediate feedback on the product quality - even at production speed. Smart signal analysis and processing toolkit was applied to the EC testing data for characterizing alongwith severities of defects. The effectiveness of the proposed technique has been demonstrated on experimental data from eddy current inspection of defects in high speed drawn steel wires. This produces a high demand of non-invasive based defect detection system that can be readily commissioned with the existing machine with small modifications.

Acknowledgement

Authors are grateful to the Director, CSIR-National Metallurgical Laboratory, Jamshedpur for his kind permission to publish the work.

References

1. A Sophian, G Y Tian DT et al (2001) Electromagnetic and eddy current NDT: a review. Insight Non-Destructive Test Cond Monit 43:302–306
2. Moulder BAA and JC (1999) Review of advances in quantitative eddy current non-destructive evaluation. J Nondestruct Eval 18:3–36
3. K J Bowker MCW and MDA (1995) Some developments in eddy current techniques for in-service inspection. Insight Non-Destructive Test Cond Monit 37:163–168
4. Palanisamy R (1991) Developments in eddy current non-destructive testing. Mater Eval 49:1158–1159
5. Rajesh SN (1993) Probability of detection models for eddy current NDE methods.
6. Li M, Lowther D, Guimarães F (2014) Robust and accurate crack reconstruction for eddy current non destructive testing. Int J Appl Electromagn Mech 45:425–430. https://doi.org/10.3233/JAE-141860
7. Saludes-rodil S, Baeyens E, Rodríguez-juan CP (2015) Unsupervised Classification of Surface Defects in Wire Rod Production Obtained by Eddy Current Sensors. 10100–10117. https://doi.org/10.3390/s150510100
8. Taylor P, Sasi B, Rao BPC, et al Research in Nondestructive Evaluation Wavelet Transform – Based Denoising Method for Processing Eddy Current Signals. 37–41. https://doi.org/10.1080/09349847.2010.488799
9. Safdarnejad S, Udpa L, Udpa SS, et al (2014) Statistical Algorithms for Eddy Current Signal and Noise Analysis. 1335:1328–1335. https://doi.org/10.1063/1.4864975
10. Rosado LS, Janeiro FM, Ramos PM, Piedade M (2013) Defect characterization with eddy current testing using nonlinear-regression feature extraction and artificial neural networks. IEEE Trans Instrum Meas 62:1207–1214. https://doi.org/10.1109/TIM.2012.2236729
11. Liu Z, Yao J, He C, et al (2018) Development of a Bidirectional-Excitation Eddy-Current Sensor With Magnetic Shielding : Detection of Subsurface Defects in Stainless Steel. IEEE Sens J 18:6203–6216. https://doi.org/10.1109/JSEN.2018.2844957

Experimental Evaluation of X-ray Digital Radiographic and Computed Tomographic System using an Indirect FPD for Non-destructive Examination

Lakshminarayana Yenumula[1,2*], Anant Mitra[1], Rajesh V Acharya[1,2], and Umesh Kumar[1]
[1]Industrial Tomography and Instrumentation Section, Bhabha Atomic Research Centre, Mumbai - 400085, India
[2]Homi Bhabha National Institute (HBNI), Anushaktinagar, Mumbai - 400094, India
*laxmany@barc.gov.in

Abstract

Integrated high-flux X-ray based Digital Radiography and Computed Tomography (DR&CT) using two-dimensional (2D) Digital Detector Array (DDA) is one of the upcoming imaging technologies for Non-destructive Evaluation (NDE) of industrial specimen. It offers acquisition of direct digital radiographic images and facilitates generation of volume tomographic data for advanced NDE analysis. Scintillator based DDAs are commercially available and are known as indirect Flat Panel Detectors (FPDs). Due to spatial and temporal anomalies and possible degradation of the FPD performance over time, it is important to periodically evaluate its performance to ensure the image quality, level of accuracy, sensitivity and long-term stability. The present paper describes evaluation of radiographic performance of an in-house developed DR&CT imaging facility with Gadolinium oxysulfide (GOS) based FPD system. Image quality parameters such as Image Lag (IL), Offset Level (OL), bad pixel distribution, Spatial Resolution (SR), Material Thickness Range (MTR), Contrast Sensitivity (CS), Signal Level (SL) and Signal-to-Noise Ratio (SNR) have been analysed. The study also includes determination of Modular Transfer Function (MTF) and Basic Spatial Resolution (SR_b) of the imaging system.

Keywords: Digital Radiography and Computed Tomography (DR&CT), Digital Detector Array (DDA), Non-destructive Evaluation (NDE), Flat Panel Detector (FPD), Material Thickness Range (MTR), Contrast Sensitivity (CS), Modular Transfer Function (MTF)

1. Introduction

Integrated high-flux X-ray based Digital Radiography and Computed Tomography (DR&CT) using two-dimensional Digital Detector Array (DDA) such as Flat Panel Detector (FPD) is one of the upcoming imaging technologies for Non-destructive Evaluation (NDE) of industrial specimen. It offers acquisition of direct digital radiographic images and facilitates generation of volume tomographic data for advanced NDE analysis. Further, image generation with FPD is almost a real-time process, with a time lapse between exposure and image display of about less than 10 seconds. Consequently, this imaging technology is highly productive and more specimens can be examined in the same amount of time than with other radiographic modalities such as film-based radiography and computed radiography.

In industrial domain, an indirect conversion FPD using terbium-doped gadolinium oxysulfide (Gd_2O_2S:Tb - GOS) scintillator coupled with amorphous silicon (a-Si) is one of the most widely used 2D DDA due to its higher Detection Quantum Efficiency (DQE) at low dose, high dynamic range and resistant to mechanical stress [1 - 6].

From a digital image interpretation standpoint, final quality of a digital image from a specific detector is an important metric. The quality of a digital image is affected by several factors involved in the entire imaging chain including exposure parameters, exposure technique, nature of the display technology, imaging software and inherent property of a detector. Some of the inherent properties of the detector which influence the image quality are Spatial Resolution (SR), Signal-to-noise Ratio (SNR), DQE, detector Image Lag (IL) (ghost images and residual images), Offset Level (OL), Burn In (BI), internal scatter radiation and bad pixels. The other metrics such as achievable Contrast Sensitivity (CS) and specific Material Thickness Range (MTR) are dependent on both the detector used as well as specimen under test [7]. Due to spatial and temporal anomalies and possible degradation of the FPD performance over time, it is important to periodically evaluate its performance to ensure the image quality, level of accuracy, sensitivity and long-term stability [8]. The testing procedure requires the usage of either the five-groove wedge or the duplex plate phantom with separate Image Quality Indicators (IQIs) [9].

The present paper describes evaluation of radiographic performance of an in-house developed DR&CT imaging facility with GOS based FPD system using duplex plate phantom. Image quality parameters have been analysedaccording to the standard ASTM E2737-10 [9]. These parameters include IL, OL, bad pixel distribution, BI, SR MTR, CS, and Signal Level (SL).The study also includes determination of Modular Transfer Function (MTF) using edge response method and Basic Spatial Resolution (SR_b) of the system with duplex wire phantom.

2. Experimental Details

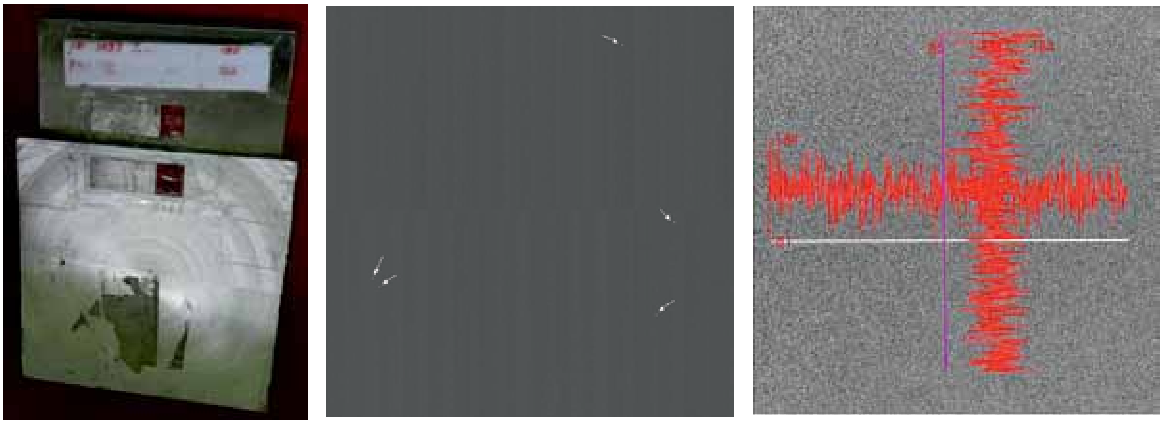

(a) (b) (c)

Figure 1 : (a) Duplex plate phantom with required IQIs positioned on the plates (one ASTM E1025 or E1742/E1742M penetrameter on each plate and one ASTM E2002 Duplex Wire IQI on the thinner plate) (b) image showing bad pixel distribution before correction (c) calibrated image (after offset, gain and bad pixel corrections) with horizontal and vertical line profiles.

Duplex plate phantom used in the present experimental study to evaluate performance of the X-ray DR&CT system with FPD is shown in Figure 1(a). The duplex plate phantom consists of two flat plates of 6 mm and 10 mm so that the thickest part of the phantom is 16 mm. The plates were constructed from Stainless Steel (Material group 1). The plates were positioned such that the second plate covered half of the first plate. The thickness of both plates together is similar to the highest material thickness that can be inspected for a given X-ray voltage. The IQIs have been positioned on the plates in accordance with the standard. One ASTM E1025 or E1742/E1742M hole-type penetrameter on each plate and one ASTM E2002 Duplex wire IQI on the thinner plate have been placed to evaluate the quality of the FPD system. The FPD used in the present study has GOS scintillator with a bit depth of 16 bits signal digitization and 200 μm pixel size. Prior to the performance testing, the FPD was calibrated for offset and gain to generate corrected images for each exposure conditions and detector settings used in the testing procedure. Besides that, bad pixel correction was also performed in accordance with standard ASTM E2597 [10]. Figure 1(b) shows the bad pixel distribution of the FPD system. It can be noted that the bad pixels have been highlighted with arrows. Figure 1(c) shows white image acquired after offset, gain and bad pixel corrections. Horizontal and vertical line profiles can be seen in the figure.

The measurements were made using a constant potential X-ray tube with focal spot size of 0.4 mm and maximum voltage of 200 kV. The phantom was placed directly on the FPD. The source-to-detector distance was 1650 mm. Table 1 reports the exposure parameters (tube voltage, current and integration time) used for the performance testing of the FPD system. The acquired digital images have been evaluated to measure IL, OL, bad pixel distribution, BI, SR MTR, CS, and SL. Further, Modular Transfer Function (MTF) and Basic Spatial Resolution (SR_b) of the system were determined using edge method and duplex wire gauge, respectively. The description of these measurements is presented below.

Offset Level (OL): For determination of OL value, the DDA response was measured with no offset or gain corrections and without radiation. But, activate the bad pixel correction. Before measurement of the OL value, the DDA was powered ON for 30 minutes to get the DDA stabilized at room temperature. One image with about 30 s integration time was captured without radiation (ImageOL). Later, a Region of Interest (ROI) of about 90% of the active area of the DDA was drawn and mean GV in the ROI was measured which represents OL.

Image Lag (IL): For determination of IL value, the DDA response was measured with no offset-correction or gain-correction but with active the pixel correction. First, the DDA was exposed with a constant dose rate with the selected energy at about 80 % of saturation Gray Value (GV) of the DDA. The lag of the detector was measured using three images: (i) an offset image ($L0$) captured without radiation (ii) an image ($L1$) captured with about 10 s total integration time (e.g., an average of 10 frames using one second frame times) and (iii) an image (L2) captured while shutting down the X-rays (e.g., With the X-rays remaining on, an average image of a sequence of images captured for about 20 s while shutting down the X-rays after approximately three seconds). After image acquisition, a ROI of about 50 x 10 pixels was drawn at the same position in all images and the mean GVs were noted. The lag was calculated using mean GVs of L1 and L2 corrected by offset image mean GV according to the following equation [9].

$$IL(\%) = \frac{GV(L2) - GV(L0)}{GV(L1) - GV(L0)} \times 100 \quad (1)$$

Bad pixel distribution: For this purpose, all relevant clusters were noted from the file supplied by the manufacturer and Bad pixel map (ImageBP) was stored.

Spatial Resolution (SR): For determination of SR value, a duplex-wire IQI was directly placed on the phantom in the region of smaller thickness (see Figure 1(a)). A line profile was created through the duplex-wire gauge such that the profile covered approximately 60 % of the width of the duplex wires. The largest wire pair with less than 20% dip resolution has been determined to obtain the SR_{min}.

Contrast Sensitivity (CS): For CS test, two hole-type IQIs were used. Each one of the IQIs was placed directly on the surface of the duplex plate phantom (one in the thinner thickness and one in the thicker thickness region). The CS was calculated by the difference in Signal due to the 2T hole divided by the noise around the hole (see Figure 1(a)) in relation to the quotient of the material thickness of the step and the penetrameter. The diameter of the hole [in pixels] was measured as Dhole. A small ROI with half of the size of the diameter Dhole was placed inside the hole. The median GV of the ROI was taken as GVmedian [hole]. Two square boxes with double the size of Dhole and four times the size of Dhole were drawn about the hole as shown in Figure 2(a). The mean GV of the area between both boxes were measured as GVmean [beside squares]. The standard deviation in that area between the boxes was measured as Sigma [beside squares]. With the total material thickness at the position of the IQI (base material + IQI thickness) MTtotal and the thickness of the IQI MTIQI the Contrast Sensitivity was determined by [9]:

$$CS(\%) = \frac{GBV}{CNR} \times \frac{MT_{IQI}}{MT_{Total}} \times 100 \quad (2)$$

where GBV is the required contrast of the hole (i.e., 2.5). This value shall be agreed between user and customer. The values for the thin and the thick region of the Duplex Plate Phantom were documented.

Material Thickness Range (MTR): maximum material thickness range was evaluated from the calculation of CNR mentioned above through the hole-type IQI in the thicker region of the duplex plate phantom. The CNR was calculated by the difference in mean GV due to the 2T hole divided by the noise around the hole. The MTR is determined by the following condition: If CNR>GBV this material thickness can be inspected and the test is passed.

Signal-to-noise Ratio (SNR): For the measurement of SNR, two ROIs of 50 x 50 pixels on the thin area (ROI 1 and ROI 2) and two ROIs on the thick area (ROI 3 and ROI 4) were drawn at the locations of the Duplex Plate Phantom as shown in Figure 2(b). The mean signal GVmean and the standard deviation (Sigma) of each ROI were measured. SNR is the quotient of both, according to the following equations [9]:

$$SNR_{thick} = \left(\frac{GV_{mean}(ROI3)}{sigma(ROI3)} + \frac{GV_{mean}(ROI4)}{sigma(ROI4)} \right) * 0.5 \quad (3)$$

$$SNR_{thin} = \left(\frac{GV_{mean}(ROI1)}{sigma(ROI1)} + \frac{GV_{mean}(ROI2)}{sigma(ROI2)} \right) * 0.5 \quad (4)$$

Signal Level (SL): The SL values for the thin and thick material were determined by the same four ROIs (ROI 1, ROI 2, ROI 3 and ROI 4) mentioned above. SL value for each ROI was obtained by the mean GV divided by the standard deviation (Sigma) as per the following equations [9]:

$$\begin{aligned} GV_{thin} &= [GV_{mean}(ROI1) + GV_{mean}(ROI2)] * 0.5 \\ GV_{thik} &= [GV_{mean}(ROI3) + GV_{mean}(ROI4)] * 0.5 \end{aligned} \quad (5)$$

Modular Transfer Function (MTF): The MTF quantifies the spatial resolution of an imaging system. The MTF can be calculated using two methods: edge method and slit method [12 - 14]. In the present study, edge method has been used as edge test objects are widely available. To test the MTF of the FPD system a specimen of thin rectangular stainless steel plate with polished edge and surface was used. The specimen was directly placed on top of the detector surface with a small tilt angle (~ 2 degrees) between the edge and the row or column of the detector pixel array. The image of the slanted edge was taken to produce the Edge Spread Function (ESF). The ESF was then differentiated to obtain the Line Spread Function (LSF). Finally, the MTF of the LSF was normalized to 1 at zero frequency. The MTF was calculated from the following equation:

$$MTF(x) = |FT\{LSF(x)\}| = \left| FT\left\{ \frac{d}{dx}[ESF(x)] \right\} \right| \quad (6)$$

3. Experimental Results and Discussion

After correcting for bad pixels, SR_b of the FPD system has been evaluated using two duplex wire IQIs. Arrangement of the duplex wire IQIs is shown in Figure 3. Figure 4 shows horizontal and vertical line profiles for evaluation and SR_b of 200 microns has been achieved. Table 1 presents exposure parameters used for the performance evaluation of the FPD system using various parameters. Table 2 shows summary of the results obtained from the experimental measurements performed with and without the duplex plate phantom. Image quality parameters of IL, OL, SR, MTR, CS, SL, SNR, MTF and SR_b were analysed to assess the performance of the FPD system. They provide knowledge about the quality characteristics of the analysed FPD system and assists in selecting the detector for a given application. Figure 2(b) presents the duplex plate phantom image with ROI 1 to ROI 4 for evaluation of signal level and SNR test parameters. In the present study, the duplex plate phantom has been designed with the highest thickness of 13 mm, so the maximum MTR achieved is 13 mm with CNR of 14.9. The SR value of 200 microns has been achieved (Figure 5). A SL of 5068 has been achieved. The FPD system presented CS and SNR of 0.64% and 92 values for thick region, respectively. The system exhibits short lag, which is a residual signal in the FPD that occurs shortly after the exposure is completed. To determine MTF, ESF and LSF were calculated. The acquired digital images were evaluated through the IQWorks v0.72 (Revision 23307) open source software. Figure 6(a) and 6(b) show ESF and LSF obtained by differentiating ESF at three different exposure conditions (100 kV, 150 kV and 200 kV). The MTF values were calculated from the LSF and normalized to 1 at zero frequency as shown in Figure 7. The MTF studies showed that this FPD gives spatial resolution of 2.75, 2.70 and 2.69 line pairs per mm at detector plane for 100 kV, 150 kV and 200 kV, respectively. These studies provide a good understanding about the behavior of the FPD system and its influence on the quality of the digital radiographs. The data will serve as reference data for the future measurements.

(a)

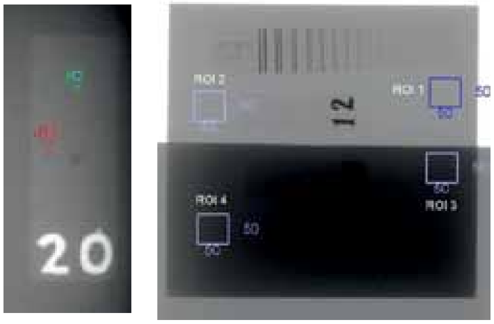

(b)

Figure 2 : (a) Determination of contrast sensitivity using hole-type penetrameter for thick region of duplex plate phantom (b) Duplex plate phantom image with ROI 1 to ROI 4 for evaluation of signal level and SNR.

Figure 3 : Arrangement of Duplex wire IQIs for evaluation of detector Basic Spatial Resolution (SR_b).

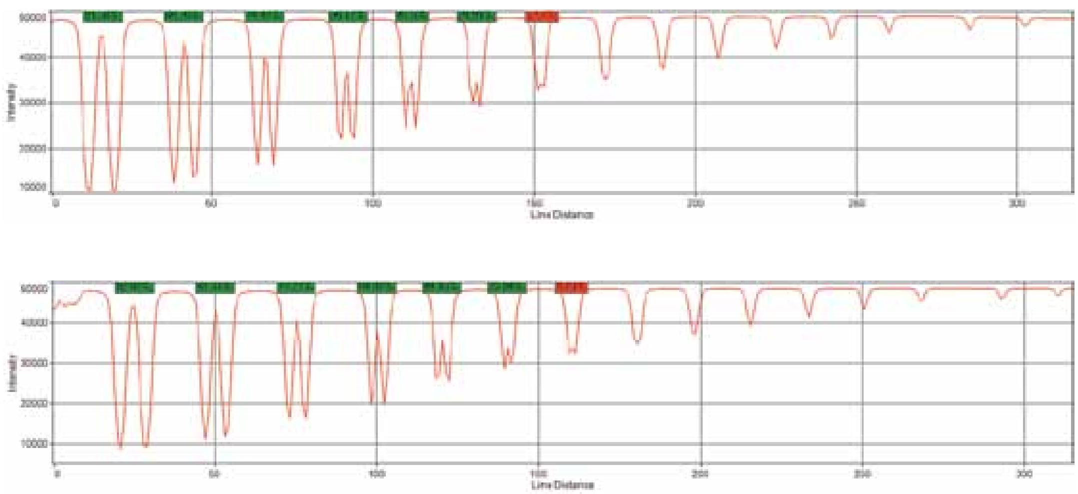

Figure 4 : Line profiles for evaluation of Basic Spatial Resolution (SR_b) of FPD (a) Horizontal profile (D7 < 20%) (b) vertical profile (D7 < 20%)

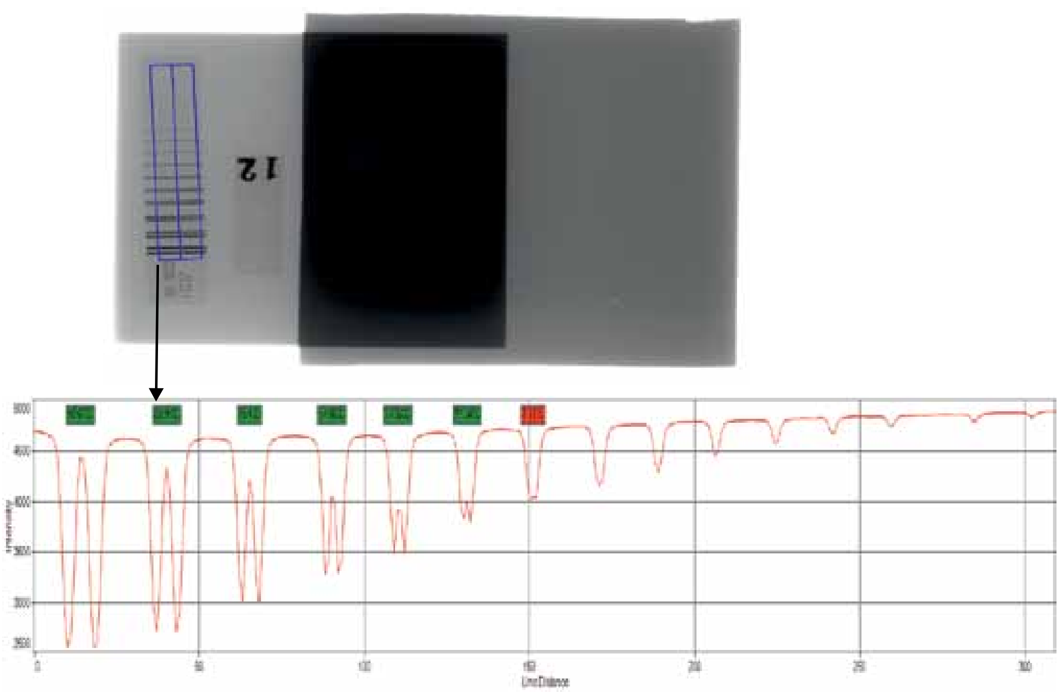

Figure 5 : Line profile showing basic spatial resolution of 200 μm (D7 < 20%) using the 200 μm pixel FPD and 0.4 mm focus X-ray tube.

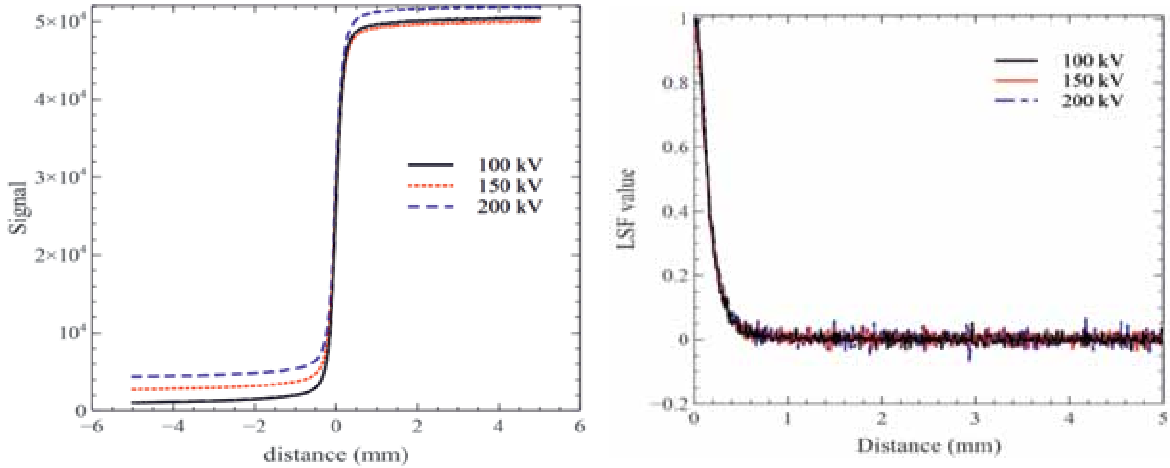

Figure 6 : (a) Edge Spread Function (ESF) at three different exposure conditions (100 kV, 150 kV and 200 kV) (b) Line Spread Function (LSF) at three different exposure conditions (100 kV, 150 kV and 200 kV).

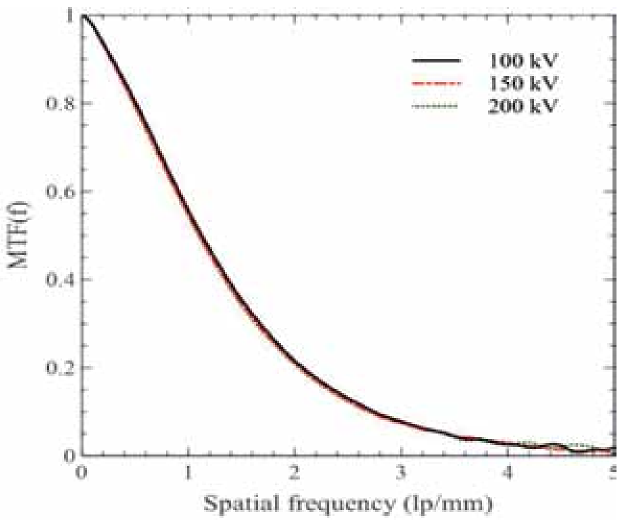

Figure 7 : Plot of MTF vs. spatial frequency at three different X-ray tube voltages.

Table 1 : Exposure parameters used for the performance evaluation of the FPD system.

FPD	Tests	X-ray tube voltage (kV_p)	Current (mA)	Integration Time (s)
GOS based FPD	IL	200	0.6	10 s
	OL	200	0.6	30 s
	MTF	100	1.7	1 s
		150	0.8	1 s
		200	0.55	1 s
	Offset	200	0.6	10 s
	Gain	200	0.6	10 s
	Other tests with phantom	200	0.6	20 s

Table 2 : Image quality parameters achieved using duplex plate phantom for the FPD system.

Image quality parameter		Result
Image Lag IL(%)		0.17%
Offset Level (OL)		5140
Bad pixel distribution		Stored the bad pixel map
Spatial Resolution (SR)		200 microns
Material Thickness Range (MTR)		13 mm
Contrast SensitivityCS(%)	Thin	0.92%
	Thick	0.64%
Signal Level (SL)	Thin	5068
	Thick	1911
Signal-to-noise Ratio(SNR)	Thin	128
	Thick	92

TECHNICAL PAPERS

4. Conclusion

This paper presents performance evaluation of an in-house developed X-ray Digital Radiography and Computed Tomography (DR&CT) imaging facility with GOS based Flat Panel Detector (FPD) system. A duplex plate phantom has been designed and fabricated to perform the quality tests as per ASTM E2737-10. Image quality parameters such as Image Lag (IL), Offset Level (OL), bad pixel distribution, Spatial Resolution (SR) Material Thickness Range (MTR), Signal-to-noise Ratio (SNR), Contrast Sensitivity (CS), and Signal Level (SL) have been analysed. Studies have been carried out to determine system Modular Transfer Function (MTF) using edge-response function. The system Basic Spatial Resolution (SR_b) has beenevaluated using duplex wire phantom. It is observed that the experimental results are in accordance with the FPD specifications and hardware limitations. The study may serve and provide typical reference data for future applications.

Acknowledgments

The authors are grateful to Dr. Pradeep Kumar Pujari, Director, Radiochemistry and Isotope Group (RC&IG), Bhabha Atomic Research Centre (BARC), Mumbai for his valuable support and constant encouragement. Thanks are also due to the technical staff of Industrial Tomography and Instrumentation Section (ITIS),BARC, Mumbai for extending help in the experimental work.

References

1. Yaffe, M. J. and Rowlands, J. A. (1997) 'X-ray detectors for digital radiography', *Physics in Medicine & Biology*. IOP Publishing, 42(1), p. 1.
2. Ewert, U., Zscherpel, U. and Bavendiek, K. (2007) 'Strategies for Film Replacement in Radiography', in *IV Conferencia Panamericana de END*.
3. Ewert, U., Zscherpel, U. and Bavendiek, K. (2008) 'Strategies for film replacement in radiography-films and digital detectors in comparison', in *Proceedings of 17th World Conference on Nondestructive Testing, Shanghai, China*, pp. 25–28.
4. Cowen, A. R., Kengyelics, S. M. and Davies, A. G. (2008) 'Solid-state, flat-panel, digital radiography detectors and their physical imaging characteristics', *Clinical radiology*. Elsevier, 63(5), pp. 487–498.
5. Oliveira, D. F. *et al.* (2010) 'Application of the digital radiography in weld inspection of gas and oil pipelines', in *Proceedings of 10th European Conference on Non-Destructive Testing–ECNDT, Moscow, Russia*, pp. 7–11.
6. Acharya, R. V, Kumar, U. and Singh, G. (2009) 'Experiences in Digital Industrial Radiography using High-Resolution A-Si Flat Panel X-Ray Detector System', *ratio*, 3(6), p. 9.
7. ASTM E2736 - 10 (2010) *Standard Guide for Digital Detector Array Radiology*.
8. de Sá Silva, A. S. (2019) 'Evaluation of digital detector arrays systems for industrial radiography', *Brazilian Journal of Radiation Sciences*, 7(2A).
9. ASTM E2737 -10 (2018) *Standard Practice for Digital Detector Array Performance Evaluation and Long-Term Stability*.
10. ASTM E2597 - 14 (2014) *Standard Practice for Manufacturing Characterization of Digital Detector Arrays*.
11. Kim, H. J. *et al.* (2003) 'Construction and characterization of an amorphous silicon flat-panel detector based on ion-shower doping process', *Nuclear Instruments and Methods in Physics Research Section A: Accelerators, Spectrometers, Detectors and Associated Equipment*. Elsevier, 505(1–2), pp. 155–158.
12. Fujita H, Tsai D-Y, Itoh T, Doi K, Morishita J, Ueda K and Ohtsuka A 1992 *IEEE Trans. Med. Imag.* 11 34-39 .
13. Samei E, Flynn M J and Reimann D A 1998 *Med, Phys.*25102-13 .
14. Buhr E and Neitzel S G n-K a U 2003 *Med, Phys.* 302323-31.

Reflection study of shear horizontal wave modes with beveled plate edges

R. Aravinth[1], NivedSuresh[2*], N. Gopalakrishnan[1] and Krishnan Balasubramanian[2]
[1]Department of Physics, National Institute of Technology Tiruchirappalli, Trichy – 620015, India
[2]Centre for Non-Destructive Evaluation, Indian Institute of Technology Madras, Chennai, India
*Corresponding author: nivedkvr@gmail.com

Abstract

The interaction of Shear Horizontal (SH) guided wave modes with beveled plate edges is investigated. This study is considered as a preliminary attempt to examine the bevel angles in Butt welds or the inclination of cracks. Reflection behaviour of SH0 wave mode is analytically and experimentally investigated. The dependency of bevel angles on the energy carried by the reflected SH0 wave modes was found out. It is found that as the bevel angle changes, the reflected SH0 wave amplitude changes. It is also observed that there are certain bevel angles at which the transmitted wave mode does not reflect. Analytical solutions were used to analyse the dependency of bevel angles. Experiments were carried out to prove these results at bevel angles of 30°, 45°, 60°, 75° and 90°. SH0 guided waves in experiments were generated using wavelength constrained PPM-EMATs.

Keywords: *Shear Horizontal (SH) waves, Bevel angle, Reflection*

1. Introduction

Guided waves are used for locating various types of defects in plates and pipes. This inspection technique can provide location andseverity of the defects[1]. Fast detection of defects in large areas scanning is the main attraction of the guided waves. An important class of guided waves is the shear horizontal (SH) waves[2].Non-destructive testing methods use Shear Horizontal waves in various areas. They are mainly used to inspect quality of plates, pipes, welded joints[3]. EMATs are the device that consists of coils and magnets to excite and receive ultrasonic waves in an electrically conducting material. In order to achieve shear horizontal wave mode excitation in Aluminium plates, based on the Lorentz force mechanism, Periodic permanent magnet (PPM-EMAT) is used along with racetrack coil [4]. PPM-EMAT has a series of alternating polarity magnets arranged consecutively. Eddy current is generated on the surface of the specimen when current passes through the racetrack coils. Magnetic field interacts with eddy current, producing the Lorentz force. The direction of Lorentz force distribution causes shear horizontal wave generation. Distance between magnets of the same polarity is the wavelength of the SH wave generated.

In this paper, we are trying to investigate the dependency of bevel angle with SH guided wave modes[5]. It has been analytically proved that various bevel angles behave differently with different incident wave modes. The objective of this paper is to investigate the dependency of shear horizontal guided wave modes with beveled plate edges. Brahim Mohammedi et al.[1] have studied the interactions of SH waves with the beveled plates analytically. In this study, we are attempting to experimentally validate the SH0 dependency with various bevel plate angles

2. Analytical Solution

In this study, we analyzed the reflection behaviour of SH0 wave mode with different bevel angles. The analyzed plate is divided into two regions by introducing a semi-circular fictitious common boundary as shown in Fig. 1. The plate is assumed to be linearly elastic, homogeneous and isotropic. From region I, an incident SH wave travel towards the artificial boundary, impinges on the beveled free end of the plate, reflects and sets up a standing wave in the bounded region II. Then the corresponding time dependent displacement fields in the region I and II are derived from Navier equations [3]. This is expressed as cartesian coordinates for the region I and in cylindrical coordinates for region II.

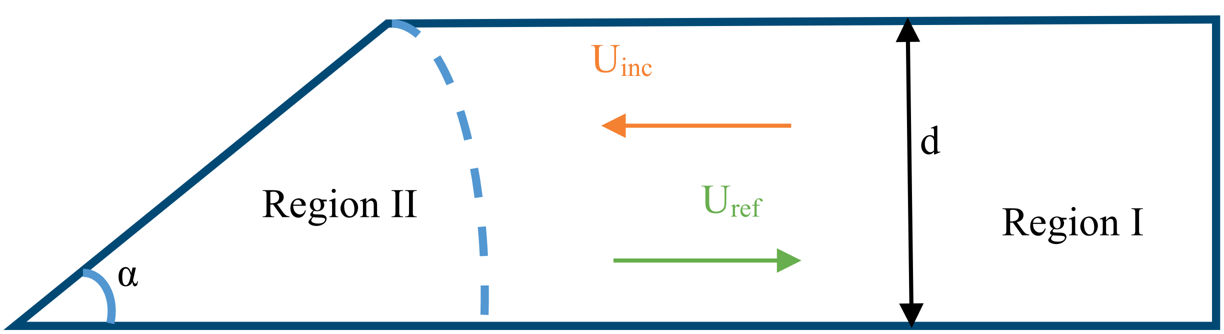

Fig. 1 : Geometry of the plate structure showing partitioned wedge and fictitious boundary

TECHNICAL PAPERS

After that, the interface continuity of displacement and stress conditions on the fictitious boundary is applied in both the regions to get the solutions. The solution of the reflected waves for the region I is expressed as an infinite sum of wave functions. For region II, the solution is represented as an infinite Bessel-Fourier sum.

After limiting the infinite series properly, this leads to a set of algebraic equations from which we will get to know the amplitudes of reflected SH wave by solving those equations[5]. Then the results are presented in terms of the ratio between the energy of the reflected mode and the energy of the incident mode for a wide range of beveled angles.

$$R_{mq} = E_{ref} / E_{inc}$$

Where m is the order of the reflected wave mode, q is the order of the incident wave mode. Now the plot is drawn for R_{m0} versus variation of the beveled edge angles.

The amplitude ratio of reflected SH0 wave mode to incident SH0 wave mode for bevel angles at the range 20 to 90 deg is shown in Fig.2. It is observed that as the angle changes, the reflection amplitude also changes and there are certain bevel angles at which the reflected SH0 wave mode completely vanished.

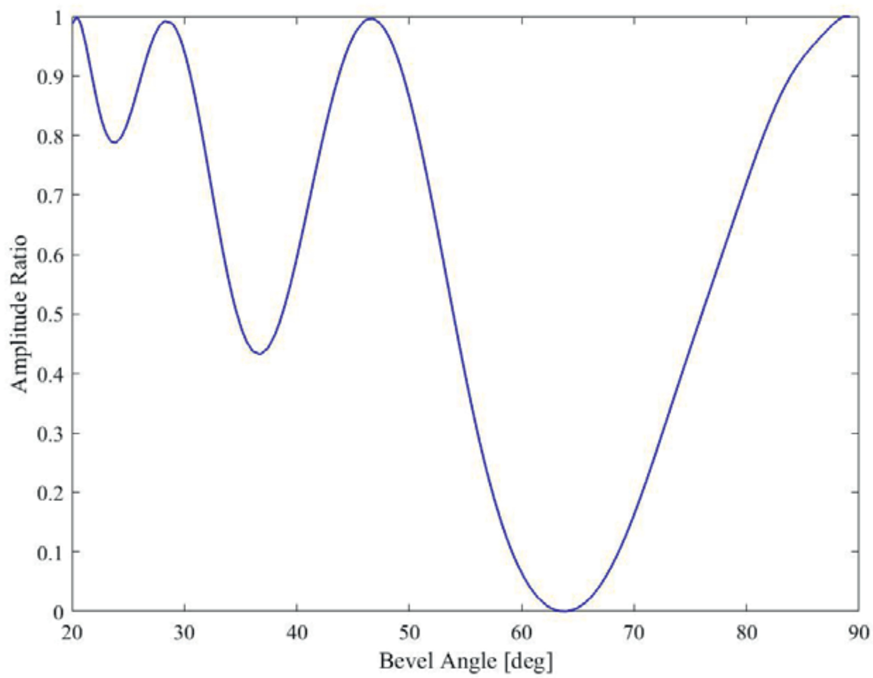

Fig. 2 : Analytical results of Amplitude ratio versus bevel edge angle

3. Experiments

4 mm Aluminium plate with bevel edge is used for this experiment. To generate and receive shear horizontal waves, PPM-EMAT is used as a transmitter and receiver. The wavelength of the PPM-EMAT used is 6.35 mm. For generating SH0 wave mode, the excitation frequency of 483 kHz is used, which is found from the phase velocity dispersion curves as shown in fig. 4. PPM-EMAT generates SH0 and is directed normally towards the beveled end of a plate [reflection paper at different angles]. From there, the reflected SH wave is received with the help of PPM-EMAT[6]. The schematic of the experiments performed is shown below in Fig. 3.1 and Fig. 3.2. The angle of the bevel plate edge varies from 300 to 900 with an increment of 150. INNERSPEC™Powerbox is used to carry out all these experiments.

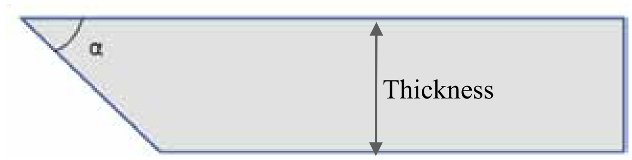

Fig. 3.1 : Front view of the bevel plate

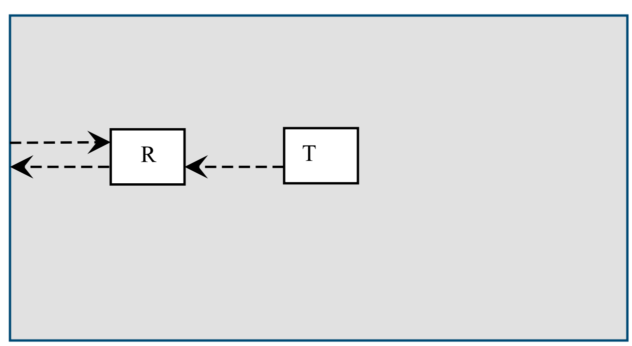

Fig. 3.2 : Top view of the bevel plate

3.1 Selection of excitation frequency from the phase velocity dispersion curves

The guided wave mode that is used in our experiment is the SH_0 mode. Wavelength constrained excitation known as Comb transduction is used here for excitation. The wavelength of excitation (λ) used is 6.35 mm. The frequency of SH_0 excitation is chosen from the phase velocity dispersion curve shown in Fig. 4[7]. The red solid curves denote symmetric modes and the blue solid curves denote antisymmetric modes. The black dashed line represents the constant wavelength line which is nothing but the wavelength of the PPM-EMAT. Then the excitation frequency of SH_0 is selected by projecting the intersection point of the SH_0 wave mode line and the constant wavelength line into the frequency axis. These two lines intersect at a frequency of 483 kHz. This is the SH_0 generation frequency for 6.35 mm wavelength in 4 mm Aluminium plate.

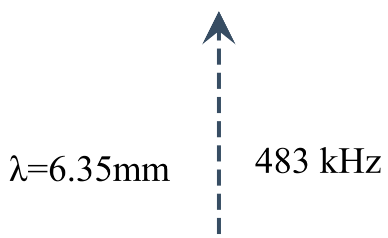

Fig. 4 : SH mode phase velocity dispersion curves for an aluminium plate of 4 mm thickness. The dashed line represents the constant wavelength line of 6.35 mm.

3.2 Results

Fig. 5. shows experimental A-scans at different bevel edge angles. The wave mode that reaches around 200 μs is the reflected SH_0 wave mode. Another wave mode that reaches around 100 μs is the incident SH_0 wave mode and the signal next to it represents the part of generated SH_1 wave mode. From Fig. 5, it is evident that up to 60° bevel edge angle, the amplitude of reflected SH_0 wave decreases. The amplitude is minimum at a 60° bevel edge angle. As the angle of bevel edge increases from 60°, the amplitude goes on increasing. The variation of the amplitude ratio of SH_0 is shown in Fig. 6.

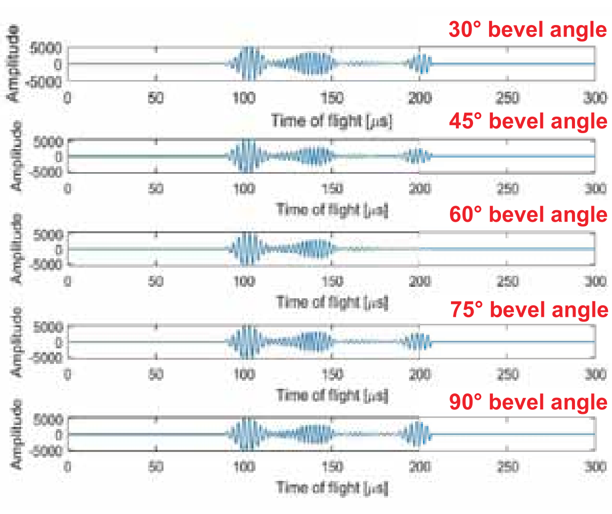

Fig. 5 : A-scans from the experiment at different bevel angles.

From the A-scans obtained from experiment, the results are defined in terms of the amplitude ratio, which is nothing but the ratio between the reflected SH_0 wave mode to the incident SH_0 wave mode.

Now the experimental results are compared with the analytical solutions as shown in Fig. 6. Most of the bevel angle experimental results, matches with the predicted analytical solutions. The slight deviation obtained in the results can be due to mode conversion from SH0 wave modes to other higher order SH wave modes or to other Lamb wave modes[8]. The analytical solution predicts the results exactly at the single frequency. The deviation in the result can be due to the presence of wide bandwidth in the incident SH0 wave mode[9].

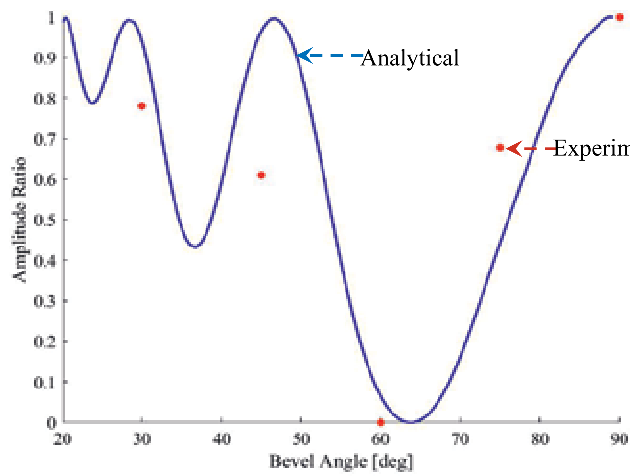

Fig. 6 :Comparison of experimental results versus analytical results

4. Conclusion

The reflection of SH0 waves by the beveled plate edge is examined through analytically and experimentally. Then the experiment is conducted on an Aluminium plate having five different bevel edge angles. It was proved that the results got through experiments agrees well with the analytical results. This study has shown the existence of critical bevel angles where the reflection SH0 wave amplitude is either 0 or 1. At critical bevel angles, where the amplitude ratio is 1, the SH0 wave mode reflects with the same incident energy without mode converting to any other wave mode. At critical bevel angles where the amplitude ratio is zero, no SH0 wave mode reflects back.

5. References

1. B. Mohammedi, N. A. Sobh, D. Abueidda, and B.-B. Aissa, "Analysis of edge defects in an elastic plate using SH-waves," *J. Mech. Sci. Technol.*, vol. 33, no. 1, pp. 87–94, Jan. 2019.
2. D. N. Alleyne and P. Cawley, "The interaction of Lamb waves with defects," *IEEE Trans. Ultrason. Ferroelectr. Freq. Control*, vol. 39, no. 3, pp. 381–397, May 1992.
3. D. Alleyne, M. J. S. Lowe, and P. Cawley, "The reflection of guided waves from circumferential Notches in pipes," *J. Acoust. Soc. Am.*, vol. 129, no. 4, pp. 1869–1880, 2011.

4. M. Hirao and H. Ogi, *EMATs for Science and Industry*. Boston, MA: Springer US, 2003.
5. Z. Abduljabbar, S. K. Datta, and A. H. Shah, “Diffraction of horizontally polarized shear waves by normal edge cracks in a plate,” *J. Appl. Phys.*, vol. 54, no. 2, pp. 461–472, Feb. 1983.
6. D. Koodalil, D. Barnoncel, P. Rajagopal, and K. Balasubramaniam, “Detection of interfacial weakness in a lap-shear joint using shear horizontal guided waves,” *NDT E Int.*, vol. 112, no. March, p. 102248, 2020.
7. J. L. Rose, “Guided wave nuances for ultrasonic nondestructive evaluation,” *IEEE Trans. Ultrason. Ferroelectr. Freq. Control*, vol. 47, no. 3, pp. 575–583, May 2000.
8. N. Suresh and K. Balasubramanian, “Shear Horizontal Mode Interaction with Plate Edge at Different Incident Angles,” p. 242, 2008.
9. N. Suresh and K. Balasubramaniam, “Quantifying the lowest remnant thickness using a novel broadband wavelength and frequency EMAT utilizing the cut-off property of guided waves,” *NDT E Int.*, p. 102313, 2020.

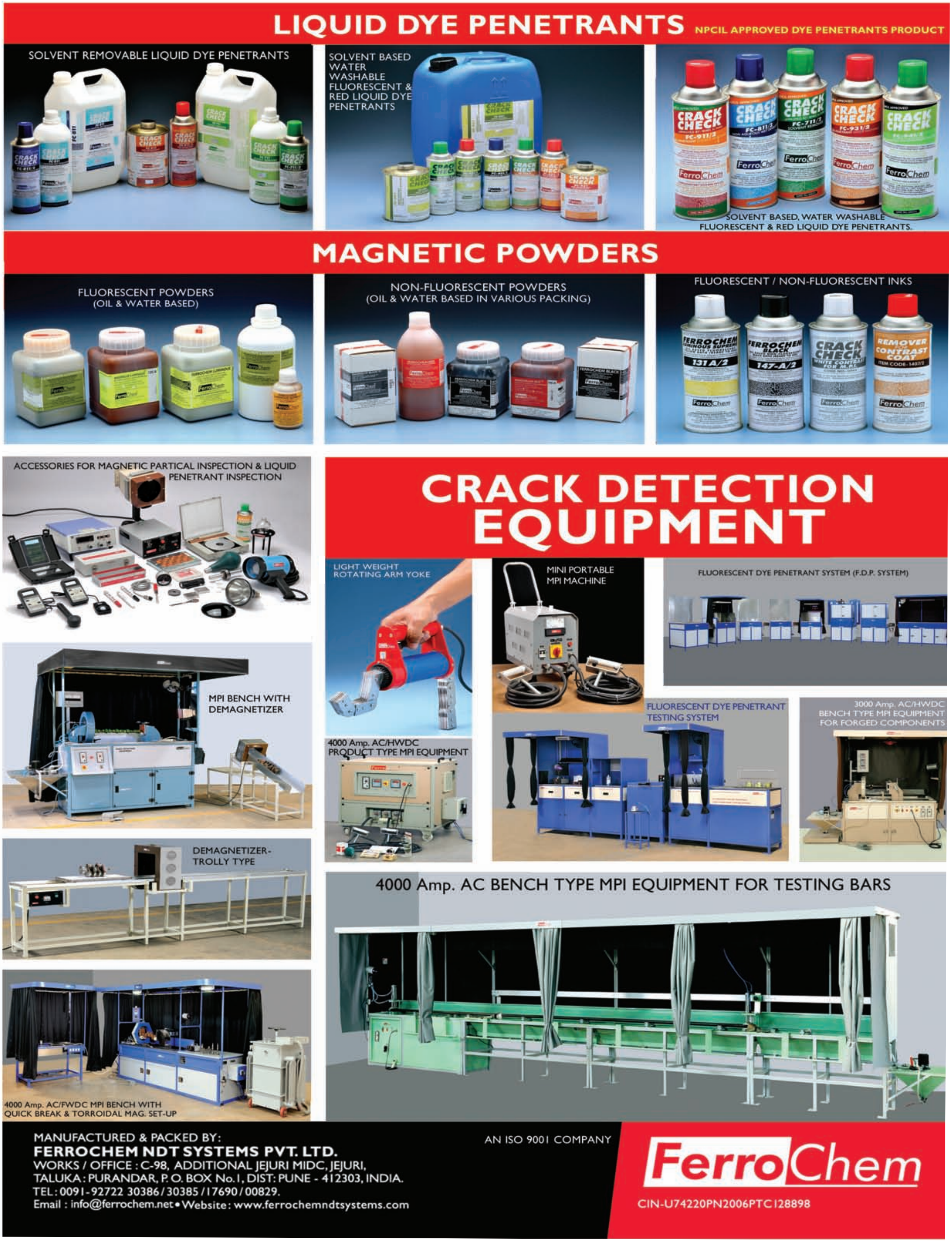
LIQUID DYE PENETRANTS
NPCIL APPROVED DYE PENETRANTS PRODUCT
SOLVENT REMOVABLE LIQUID DYE PENETRANTS
SOLVENT BASED WATER WASHABLE FLUORESCENT & RED LIQUID DYE PENETRANTS
SOLVENT BASED, WATER WASHABLE FLUORESCENT & RED LIQUID DYE PENETRANTS.
MAGNETIC POWDERS
FLUORESCENT POWDERS (OIL & WATER BASED)
NON-FLUORESCENT POWDERS (OIL & WATER BASED IN VARIOUS PACKING)
FLUORESCENT / NON-FLUORESCENT INKS
ACCESSORIES FOR MAGNETIC PARTICAL INSPECTION & LIQUID PENETRANT INSPECTION
CRACK DETECTION EQUIPMENT
LIGHT WEIGHT ROTATING ARM YOKE
MINI PORTABLE MPI MACHINE
FLUORESCENT DYE PENETRANT SYSTEM (F.D.P. SYSTEM)
MPI BENCH WITH DEMAGNETIZER
4000 Amp. AC/HWDC PRODUCT TYPE MPI EQUIPMENT
FLUORESCENT DYE PENETRANT TESTING SYSTEM
3000 Amp. AC/HWDC BENCH TYPE MPI EQUIPMENT FOR FORGED COMPONENTS
DEMAGNETIZER-TROLLY TYPE
4000 Amp. AC BENCH TYPE MPI EQUIPMENT FOR TESTING BARS
4000 Amp. AC/FWDC MPI BENCH WITH QUICK BREAK & TORROIDAL MAG. SET-UP
MANUFACTURED & PACKED BY:
FERROCHEM NDT SYSTEMS PVT. LTD.
WORKS / OFFICE : C-98, ADDITIONAL JEJURI MIDC, JEJURI,
TALUKA : PURANDAR, P. O. BOX No. 1, DIST: PUNE - 412303, INDIA.
TEL : 0091-92722 30386 / 30385 / 17690 / 00829.
Email : info@ferrochem.net • Website : www.ferrochemndtsystems.com
AN ISO 9001 COMPANY
FerroChem
CIN-U74220PN2006PTC128898

NGC/NCB Office Bearer's List

NATIONAL GOVERNING COUNCIL MEMBER'S LIST (NGC)

1. Dr. B. Venkatraman
President – ISNT
Mob: 9443638974
bvenkat@igcar.gov.in
qadbvr@gmail.com

2. Shri Diwakar D. Joshi
President – Elect -ISNT
Mob: 9822263475
diwakarj@gmail.com

3. Dr. Krishnan Balasubramaniam
Vice President – ISNT
Mob: 9840200369
balas@iitm.ac.in

4. Dr. Jaiteerth R. Joshi
Vice President – ISNT
Mob: 9440049272
joshidrdl@gmail.com

5. Shri Rajul R. Parikh
Vice President – ISNT
Mob: 9820192953
rajulparikh@eecindia.com

6. Shri Samir K. Choksi
Hon. Gen. Secretary - ISNT
Mob: 9821011113
Choksiindia@yahoo.co.in
samir.choksi@choksiworld.com

7. Shri Bikash Ghose
Hon. Jt. Secretary - ISNT
Mob: 9890127524
bikashghose@gmail.com

8. Shri Nerurkar K.A
Hon. Treasurer - ISNT
Mob: 9822525518
pradeepndt@vsnl.net

9. Shri S. Viswanathan
Hon. Co-Treasurer –ISNT
Mob: 9894945482
viswa@igcar.gov.in

10. Shri R.J. Pardikar
Immediate Past President – ISNT
Mob: 9003096843
r.j.pardikar@gmail.com

MEMBERS

11. Shri Anil V. Jain
12. Shri Anandan. P
13. Shri V. Deepesh
14. Shri Dharmveer Singh
15. Shri R.G. Ganesan
16. Prof. S. Gopalakrishnan
17. Shri S. Hari Krishna
18. Shri G. Levin
19. Shri V. Manoharan
20. Shri P. Mohan
21. Shri Mukesh Arora
22. Ms. Menaka. M
23. Ms. Navita Gupta
24. Shri Bhausaheb Krishnaji Pangare
25. Shri Partha Pratim Brahma
26. Dr. Ravibabu Mulaveesala
27. Shri Sadasivan. N
28. Ms. Sangita Kapote
29. Shri Shashidar Pallaki
30. Shri M. S. Shendkar
31. Shri Uday Kale
32. Shri Umakanthan Anand
33. Dr. Venugopal. V
34. Shri M.N.V. Viswanath
35. Shri M.S. Viswanathan
36. Shri R. Vivek

PERMANENT INVITEE

37. Shri G. Ramachandran

PAST PRESIDENTS

38. Shri V.R. Deenadayalu
39. Shri K. Balaramamoorthy
40. Shri Ramesh B. Parikh
41. Shri A. Srinivasulu
42. Dr. Baldev Raj
43. Shri D.M. Mehta
44. Shri K. Viswanathan
45. Shri S. I. Sanklecha
46. Shri Dilip P. Takbhate
47. Shri K. Thambithurai
48. Dr. P. Kalyanasundaram
49. Shri V. Pari
50. Shri D.J. Varde

EX-OFFICIO MEMBERS

51. Dr.M.T.Shyamsunder- Chairman,NCB
52. Dr. P. P. Nanekar Hon.Secretary–NCB-ISNT
53. Shri S.Viswanathan Hon.Treasurer–NCB-ISNT
54. Shri T. Loganathan Controller of Examinations, NCB - ISNT
55. Dr. Krishnan Balasubramaniam President - QUNEST Foundation
56. Shri V. Pari Member-Secretary,QUNESTFdn.
57. Dr. P. Kalyanasundaram Hon.Treasurer–QUNEST–Fdn.

NATIONAL CERTIFICATION BOARD MEMBER'S LIST (NCB)

1. Dr. M.T. Shyamsunder
2. Shri P.P. Nanekar
3. Shri T. Loganathan
4. Shri S. Viswanathan

REGIONAL CONTROLLER OF EXAMS

5. Shri A.K. Chandra
6. Shri S.R. Ravindran
7. Shri Jayaprakash Hiremath

PATRON

8. Shri K. Balaramamoorthy

MEMBERS

9 Shri. R.B. Bhardwaj
10. Shri V. Manoharan
11. Shri Avinash U. Sonawane
12. Shri R. Sundar
13. Shri Phani Babu
14. Shri Dilip Gatti
15. Shri ME. K.A Nerurkar
16. Shri Bikash Ghose
18. Shri Chintamani Khade
19. Shri G.V.S. Hemantha Rao
20. Shri. Uday B Kale
21. Shri Sadasivan. N
22. Shri. Vikas Neeraj
23. Smt. Navita Gupta
24. Shri M. Venkata Reddy

EX-OFFICIO MEMBERS

25. Dr. B. Venkatraman
26. Shri Diwakar D. Joshi
27. Dr. Krishnan Balasubramaniam
28. Shri. Jaiteeth Joshi
29. Shri. P. Mohan
30. Shri Nerurkar K.A
31. Shri. V. Pari

CHAPTER REPRESENTATION

32.Dr. Paritosh Nanekar
33. Mr. G. Ramachandran
34. Mr. Sunil Gophan
35. Dr. Jaiteerth Joshi